NASA CONTRACTOR REPORT

NASA CR-1693

NASA CR-1693

FLOW AND ACOUSTIC CHARACTERISTICS OF SUBSONIC AND SUPERSONIC JETS FROM CONVERGENT NOZZLE

by H. T. Nagamatsu, R. E. Sheer, Jr., and M. S. Gill

Prepared by
GENERAL ELECTRIC RESEARCH AND DEVELOPMENT CENTER
Schenectady, N. Y.
for

NATIONAL AERONAUTICS AND SPACE ADMINISTRATION • WASHINGTON, D. C. • DECEMBER 1970

1. Report No. NASA CR-1693	2. Government Accession No.	3. Recipient's Catalog No.
4. Title and Subtitle FLOW AND ACOUSTIC CHARACTERISTICS OF SUBSONIC AND SUPERSONIC JETS FROM CONVERGENT NOZZLE		5. Report Date December 1970 6. Performing Organization Code
7. Author(s) H. T. Nagamatsu, R. E. Sheer, Jr., and M.S. Gill		8. Performing Organization Report No.
9. Performing Organization Name and Address General Electric Research & Development Center Schenectady, New York		10. Work Unit No. 11. Contract or Grant No. NASW-1784
12. Sponsoring Agency Name and Address National Aeronautics & Space Administration Washington, D. C. 20546		13. Type of Report and Period Covered Contractor Report 14. Sponsoring Agency Code
15. Supplementary Notes		

16. Abstract

Convergent and parallel flow nozzles were used to study the flow and acoustic characteristics of subsonic and supersonic jets. For subsonic jets the core region extended 5 diameters from the jet exit and for a Mach number of 1.4 the sonic point was located at 13.7 diameters. The subsonic turbulent velocity decay region for both types of jets were similar. Peak impact pressure fluctuations on the axis occurred at approximately 9 diameters for subsonic jets and for supersonic jets the peak was located just ahead of the sonic point. Directivities for the subsonic jets were similar with the maximum sound pressure level at 19.1° from the jet axis and then decreasing with increasing angle. For supersonic jets the sound pressure level was nearly constant over most of the angular positions. The power spectra for subsonic jets were similar with the peak power occuring at 4 kHz. For a Mach 1.4 jet the peak power occurred at 5 kHz. Near field sound pressure level distributions were quite similar for subsonic jets, but for supersonic jets were quite different. Overall sound power levels were compared with the subsonic theory of Lighthill and supersonic theory of Nagamatsu and Horvay.

17. Key Words (Selected by Author(s))
Convergent parallel flow nozzles
subsonic supersonic jets
Directivities power spectra

18. Distribution Statement
Unclassified - Unlimited

19. Security Classif. (of this report)	20. Security Classif. (of this page)	21. No. of Pages	22. Price*
Unclassified	Unclassified	80	$3.00

*For sale by the National Technical Information Service, Springfield, Virginia 22151

FOREWORD

This report was prepared under contract No. NASW-1784 for NASA Headquarters, Office of Advanced Research and Technology, Research Division, under the technical direction of Mr. I.R. Schwartz. The work was conducted at the Mechanical Engineering Laboratory, General Electric Research and Development Center in Schenectady, New York.

SUMMARY

Convergent and parallel flow nozzles were used with a room temperature air supply to study the aerodynamic and acoustic characteristics of subsonic and supersonic jets. For subsonic jets the core region extended to approximately 5 diameters from the jet exit and for a Mach number of 1.4 the sonic point was located at 13.7 diameters. The subsonic turbulent velocity decay region for both subsonic and supersonic jets were similar. Peak impact pressure fluctuations on the axis occurred at approximately 9 diameters for subsonic jets and for supersonic jets the peak was located just ahead of the sonic point.

The directivities for the subsonic jets were similar with the maximum sound pressure level at 19.1° from the jet axis and the sound pressure decreased monotonically with increasing angle. But for supersonic jets the sound pressure level was nearly constant over most of the angular positions. The power spectra for subsonic jets were similar with the peak power occurring at approximately 4 kHz, and for a Mach 1.4 jet the peak power occurred at a frequency of 5 kHz. Near field sound pressure level distributions were quite similar for subsonic jets. But for supersonic jets the sound pressure distributions were quite different. From these near field measurements the overall acoustic power levels were determined and the values agreed with the far field measurements for the supersonic jets. Overall sound power levels were compared with the subsonic theory of Lighthill and supersonic theory of Nagamatsu and Horvay. The exponents α and β in this theory were evaluated for convergent and parallel flow nozzles as functions of the jet Mach number.

TABLE OF CONTENTS

TABLE OF CONTENTS (Continued)

LIST OF FIGURES

LIST OF FIGURES (Continued)

LIST OF FIGURES (Continued)

LIST OF SYMBOLS

A	cross sectional area
B&K	Bruel and Kjaer
c	velocity of sound
c_a	velocity of sound in ambient air
c_j	velocity of sound in jet
D	jet diameter
db	decibel
$F(M_j)$	function in Nagamatsu-Horvay theory
I	acoustic intensity
kHz	frequency in 1000 cycles per second
ℓ_c	jet core length
ℓ_s	supersonic length
L_s	non dimensionalized supersonic length, ℓ_s/D
L_w	overall sound power level in db
m	mass flux
M	Mach number
M_j	jet Mach number
p_a	ambient pressure
p_o	total pressure
p_o'	impact pressure after normal shock
$\bar{p}$	rms pressure
r	radius from jet centerline
R	gas constant
°R	degree Rankine
T	static temperature
T_o	total temperature

T_{t_j}	jet total temperature
U_j	jet velocity
v	velocity
w	sound power per unit length
w_d	sound power per unit diameter length
w_m	maximum sound power per unit length
W	sound power
W_o	reference sound power, 10^{-13} watts
x	axial distance from jet exit
α	exponent for sound power per unit length at jet exit
β	exponent for sound power per unit length at sonic point
γ	ratio of specific heats
ρ_a	density of ambient air
ρ_j	density of jet
θ	angle

1.0 INTRODUCTION

With the development of the large jet engines necessary for the supersonic transport airplanes, the supersonic exhaust velocities have made the problem of jet exhaust noise during take-offs quite critical around the airports located in metropolitan areas of the world. In order to reduce this exhaust noise, some knowledge of the mechanism and location of the noise sources in a supersonic jet must be obtained. But, even for subsonic jets, the actual location of the noise sources within the jet from the turbulent fluctuations has not been well defined. To apply Lighthill's theory[1,2], which relates the noise radiation to the characteristics of the turbulence within the jet, it is necessary to know the distribution of the fluctuating stress tensor in the flow field to determine the distribution of the acoustic radiation from the jet. But for supersonic jets, the available experimental data is very limited and the relationship between the noise generation from the supersonic region and the radiation to the far field is not too well understood. The present investigation was undertaken to obtain additional flow and acoustic information from subsonic to supersonic jet exhaust velocities for the purpose of determining the differences and similarities in the acoustic characteristics of subsonic and supersonic jets. It was also hoped that with better knowledge regarding the source of acoustic radiation from supersonic jets an efficient method of reducing the jet exhaust noise will be developed.

One of the early experimental studies of subsonic jets with different gases was conducted by Lassiter and Hubbard[3] to evaluate some of the effects of jet velocity, density, turbulence level, and jet diameter on the noise generated by subsonic jets. The exit Mach number was 0.9 with air, helium, and freon, with exit velocities of 928, 2620, and 415 ft/sec respectively. With helium the exhaust Mach number relative to the ambient air velocity of sound is supersonic. Due to this supersonic exit Mach number for helium, the location of the peak overall sound pressure level from the jet axis was increased from 16° for air to approximately 42° for helium. The noise intensity was found to increase by a greater amount with increases in the jet velocity and turbulence level and by a smaller amount with increases in jet diameter and exit gas density. They also showed that the noise generated by a turbojet engine was closely related to that generated by simple jet models.

The same authors in Ref. 4 extended the experimental investigation of the plain jet to supersonic exhaust velocities at various temperatures of the air. By placing the microphone at a radial location of 2 diameters from the nozzle exit and moving it along the jet axis, the overall sound pressure levels were determined over a jet exhaust velocity range of

600 to 1870 ft/sec. for stagnation temperature of 1660°R. At the lowest jet velocity the peak pressure fluctuations were nearly constant over an initial distance of 6 diameters before decreasing. As the jet velocity was increased the location of the peak pressure fluctuations moved farther from the jet exit and there was an appreciable increase in the pressure fluctuations from the jet exit to the peak location. For supersonic velocities with the convergent nozzle, a high intensity, discrete-frequency component, screech, phenomenon was observed. By the use of four small secondary air jets impinging at the periphery of the primary jet slightly downstream of the throat, the supersonic region with shock diamonds was decreased in length. The overall sound pressure fluctuations from the plain jet was decreased appreciably and the discrete frequency component was eliminated.

Gerrard[5] obtained the sound field measurements from a one inch diameter jet issuing from a pipe to investigate the theoretical predictions of Lighthill[1,2] on aerodynamic noise. Acoustic information was obtained over a jet Mach number range of 0.3 to 1.0 and over a wide frequency band of 30 Hz to 10 kHz. The lines of constant intensity for fixed frequencies were determined for different Mach numbers and the results indicated that at a given frequency the apparent source was located farther from the jet orifice at higher velocities. Lower frequency sources appeared farther downstream than ones of higher frequency. Spectra of acoustic power output per 1/3 octave band were determined over a Mach number range of 0.316 to 1.0 and the spectra were all quite similar with the maximum power output at approximately 4 kHz. The acoustic efficiency of the jet was found to be small and the observed noise field was in qualitative agreement with the Lighthill theory[1,2].

Mollo-Christensen and associates[6,7] investigated the jet flow characteristics and far-field noise spectra and directivity patterns for jet diameters of 0.5, 1.0 and 1.5 in. and for jet Mach numbers of 0.6, 0.8 and 0.9. From the stagnation pressure measurements, the Mach number distributions across the jet were determined at various locations from the jet exit. With the smallest diameter the laminar core was the longest. The contours of constant rms pressure fluctuation in the far-field were determined for different jet Mach numbers, and the peak pressures were located at approximately 20° from the jet axis, which agreed with that observed by Lassiter and Hubbard[3]. Contours of constant rms pressure for high frequencies indicated the peak pressures at approximately 50° angular position and for low frequencies the peak rms pressures were at 20° position. These results are in qualitative agreement with that observed by Gerrard[5] for subsonic jets.

Various experimental investigations[8-12] have been conducted with hot-wires to determine the characteristics of turbulence within subsonic jets which had been shown by Lighthill to be

the source of acoustic radiation. Laurence[8] investigated with hot-wire anemometers the intensity of turbulence, correlation coefficients, and the spectra of turbulence in a 3.5 in. diameter free jet at Mach numbers of 0.2 to 0.7. The characteristics of the turbulence in the mixing region of a one inch diameter jet were investigated with hot wires by Davies and colleagues[9]. For a distance of six or eight nozzle diameters of the flow the turbulence measurements indicated that there were well-defined relationships. Chu in Ref. 10 used a hot-wire anemometer to measure the turbulence in a subsonic jet in order to estimate the characteristics of the noise generated by a unit volume of turbulence in the mixing region. To accomplish this, two-point space-time correlations of both the turbulent velocities and the square of these velocities were obtained. Davies and colleagues[11] have studied the pressure field associated with the turbulent shear flows from jets with hot wires. They were able to separate the hot-wire output into that due to the turbulent and pressure field components and from these measurements determined the radial distribution of turbulent and pressure intensity for a subsonic jet. Hot-wire measurements of fluctuating turbulent stresses in the mixing layer of a two-dimensional jet were made by Jones[12] to aid in understanding the aerodynamic noise generation from subsonic jets.

The noise from a supersonic jet has been studied by various investigators with small jets. Powell[13] was able to correlate the loud "screech" from room temperature supersonic jets with the schlieren photographs of the jets. These photographs indicated that the sound waves of ultrasonic frequency were caused by the transition of the initially laminar boundary layer to turbulence. The near-field and far-field noise surveys for solid-fuel rockets were conducted by Mayes and colleagues[14]. With these rockets the exhaust velocities were close to 8500 ft/sec. but the jet Mach number varied from 2.65 to 4.07. Near field surveys indicated that the sound pressure level increased monotonically from the jet exit and the highest pressure occurred at about 20 exit diameters downstream of the nozzle near the transition from supersonic to subsonic flow. Potter and Jones in Ref. 15 observed the same phenomenon for a small nitrogen jet at room temperature with an exit Mach number of 2.5 and corresponding velocity of 1800 ft/sec. They were able to determine the acoustic power generated per unit length of the jet flow by the use of a large reverberation room. The acoustic power distribution increased from the jet exit and the peak acoustic power generation occurred at approximately 20 diameters downstream, which was just ahead of the sonic location.

Experimental and analytical studies of axisymmetric free jets have been made by Warren[16], Love[17], and Eggers[18]. Using heated air jets Warren obtained the velocity and temperature distributions over a Mach number range of 0.69 to 2.6, where the supersonic jet Mach numbers were obtained with contoured nozzles

to produce uniform parallel flow at the exit. Love and colleagues investigated the effects of jet Mach number, nozzle divergence angle, and jet static-pressure ratio upon the jet structure, jet wavelength, and the shape and curvature of the jet boundary. Experimental observations were made to correlate with the characteristic solutions for the supersonic jets. Eggers determined the velocity profiles and eddy viscosity distributions for a Mach 2.22 jet exhausting into quiescent air from a contoured nozzle. Near-field and far-field noise measurements were made by Mayes[19] of the supersonic jet with thrust rating of approximately 475,000 lbs. This exhaust jet was from the large thermal structures tunnel at Langley Field. For these tests the exhaust velocity was in the range of 2800 ft/sec. and temperature of 420°R. The near-field noise results indicated that the maximum sound pressure levels in the high-frequency bands were greatest near the jet exit. Dosanjh[20] and his colleagues have been investigating the sound generation and reduction of noise from small supersonic jets. By using radially impinging annular jet flow, the total acoustic power emitted by a supersonic jet from an axisymmetric converging nozzle was decreased by 3.5 db and the shock structure in the main jet flow was radically altered.

The primary purpose of the present investigation was to obtain the flow and acoustic characteristics of subsonic and supersonic jets and to determine the differences between these jets. Experimental aerodynamic and acoustic data were obtained from axisymmetrical convergent nozzle operated over a range of pressure ratio with corresponding range of Mach number from 0.60 to 1.40. Axial surveys were conducted with impact pressure and total temperature probes, and with a piezo-electric impact pressure probe to determine the total pressure fluctuations along the jet axis. Acoustic measurements were made with microphone rotated on a 10-ft. radius from the nozzle exit to determine the far-field acoustic characteristics and axial surveys with the microphone placed at various radial distances from the jet periphery to measure the near-field characteristics. Both aerodynamic and acoustic experimental data were correlated with the subsonic jet noise theory of Lighthill[1,2] and the supersonic theory of Nagamatsu and Horvay[21].

2.0 EXPERIMENTAL FACILITIES AND PROCEDURES

2.1 Air Supply and Flow Control System

For the flow and acoustic studies of jets exhausting to atmosphere, the compressed air was supplied by a large reciprocating four-stage compressor with an 800 hp motor. There were two of these compressors available and both of them were required for jet Mach numbers greater than 1.4 with 2 in. diameter throat. With both compressors 8 lbs/sec. at 250 psig can be supplied continuously. The compressed air was passed through after-coolers, large oil separators and settling tanks. A photograph of the jet exhaust test facility and part of the building housing the compressors and showing the cooling tower is shown in Fig. 1. From the settling tanks the compressed air flowed through a 6 in. pipe with an orifice flow meter to the Fisher pressure control system installed just inside the building, and then through the 4 in. pipe shown in Fig. 1. With the automatic air flow control system, it was possible to maintain the pressure at preselected constant operating values in the 12 in. diameter reservoir or plenum chamber located at the end of the 60 ft. long 4 in. diameter pipe as indicated in Figs. 1 and 2. During the tests the reservoir pressure was held constant within 0.1 psi by the Fisher pressure regulator. A large gas fired air heater is available to heat the air to 1260°R at 500 psig for hot jet experiments. For these initial investigations of the plain jet, the unheated air was used to simplify the instrumentation for obtaining flow data in the jet at various distances from the jet exit.

2.2 Nozzle and Test Facility

A conical convergent nozzle and a contoured parallel flow nozzle for an exit Mach number of 1.5 with throat diameter of 2 in. were used in the present studies. The majority of the tests were conducted with the convergent nozzle and the acoustic and flow results with the contoured nozzle with exit Mach number of 1.5 are presented in Refs. 22 and 23. The initial investigations[22] were conducted with the jet located adjacent to the building but to minimize the acoustic interferences from the structure the jet was moved 60 ft. away from the building, cf. Figs. 1 and 2. These nozzles were attached to the contraction section of the 12 in. diameter plenum chamber. Both the static pressure and total temperature of the compressed air were measured in this plenum chamber, which contained screens to break large scale turbulent eddies into smaller eddies. To minimize the ground reflection effects, the jet axis was located approximately 36 jet diameters above the ground.

A trolley system as shown in Fig. 1 with rails 20 ft. apart was used to conduct axial surveys of the jets with impact pressure, total temperature, and piezo-electric total pressure

probes. Also, it was possible to survey along the jet with the microphone placed at various radial distances from the nozzle exit. Stands were placed at both ends of the trolley for the purpose of obtaining schlieren and shadowgraph photographs of the jets at various distances from the jet exit.

2.3 Instrumentation

Static pressures for the convergent nozzle and in the settling section ahead of the nozzle were measured with a 14 in. diameter Heisse pressure gage. High impact pressures were measured with the Heisse gage and for low impact pressures on the jet axis at large distances downstream of the jet exit a mercury manometer was used. For each test the ambient pressure was read from a mercury barometer. Since the jet flow can be maintained continuously with the compressors, all static and impact pressures were read after the pressures were stabilized.

The total temperature in the plenum chamber was determined by means of a chromel-alumel thermocouple or an Ashcroft dial thermometer. A thermocouple was used in the total temperature probe for the axial surveys along the jet axis. The outputs from both of these thermocouples were recorded simultaneously on a Minneapollis-Honeywell visicorder. These thermocouples were calibrated over the range of total temperatures encountered in the jet flow. A thermometer was placed below the plenum chamber to measure the ambient air temperature during the tests.

Acoustical instrumentation consisted of a B&K 1/2 inch free field response condenser microphone with a cathode follower, which had a frequency response of 20 Hz to 40 kHz. The microphone was calibrated before each run with a B&K piston phone calibrator which produced an oscillating dynamic pressure of 124 db re .0002 microbar at 250 Hz. For far-field acoustic measurements the microphone was placed in the plane of the jet axis at 8 angular positions on a 10 ft. radius from the jet exit as indicated in Figs. 1 and 2. The output of the microphone was connected to a Ballantine true rms voltmeter, B&K sound level meter, and General Radio data tape recorder which had a frequency response range from 15 Hz to 16 kHz. For a few selected tests a Consolidated Electrodynamics Corporation tape recorder was used which had a frequency response of 0.1 to 100 kHz. These experiments were conducted to determine the acoustic power distribution over the frequency range of 16 to 80 kHz. The Ballantine true rms voltmeter had a flat frequency response better than 200 kHz. The recordings were analyzed using a B&K 1/3 octave-band analyzer coupled to a Hall squaring circuit and a digital integrating voltmeter. This procedure results in a mean square pressure determination over 5-second periods for each analyzer band as discussed in Ref. 22.

With the available optical instrumentation, schlieren, shadowgraph, and interferometer photographs of the jet flow can be obtained. The field of view for the interferometer is 2 in. diameter with either green or white light sources. By using a single beam of the interferometer it is possible to obtain shadowgraph or schlieren photographs. Two 12 in. diameter parabolic mirrors with a focal length of 8 ft. are available for mounting on the moveable trolley. For this system either a steady light source or a spark source with 0.4 microsecond duration is available.

2.4 Procedure

Two separate runs were made at each selected reservoir pressure with the convergent nozzle to obtain the acoustics and flow information. The reservoir pressures for the nozzle were selected to produce jet flow Mach numbers from 0.60 to 1.40. For each nozzle pressure ratio, which is the ratio of reservoir to ambient pressure, the Fisher flow regulator was adjusted to maintain constant reservoir pressure for the duration of the run. The nozzle and reservoir pressures and the total temperature in the reservoir were recorded after the jet flow had attained equilibrium condition. Total pressure and total temperature surveys along the axis of the jet were made from the nozzle exit to 40 nozzle diameters downstream. The probes were held at a given axial position until the total pressure or the total temperatures had reached equilibrium value. These axial surveys were conducted only when the ambient wind velocity indicated on a wind velocity meter was less than 10 mph. The ambient temperature and pressure were recorded for each test.

The far-field acoustic measurements were made with the microphone placed at eight angular positions in a horizontal plane at a fixed 10 ft. radius from the jet exit as shown in Figs. 1 and 2. Before each test the microphone was calibrated with the B&K piston phone calibrator. After the jet flow was established, the microphone was held in each angular position for approximately one minute to record the microphone output with the tape recorder and obtain the rms voltmeter and B&K sound pressure level meter readings. Axial near field surveys were made with two microphones located at a radial distance of 2 and 4 diameters from the nozzle exit as indicated in Fig. 2. A second series of near field measurements were made with microphones at 3 and 8 diameters. For these near-field surveys the outputs from the microphones were connected to the Ballantine rms voltmeter to obtain the sound pressure level at each location in db re .0002 microbar.

To determine the total pressure fluctuations along the center line of the jet, a 1/4 in. diameter "Kistler" quartz pressure transducer with the probe face normal to the jet was mounted on the trolley with a long sting holding the probe. The output

from the pressure probe was connected to the Ballantine rms voltmeter to determine the magnitude of the total pressure fluctuations in mv. The total pressure fluctuations were measured from the jet exit to 40 diameters downstream over a jet Mach number range of 0.60 to 1.40.

3.0 RESULTS AND DISCUSSION

3.1 Aerodynamics

3.1.1 Optical Results

An interferometer with a 2 in. field of view with green and white light source was used to obtain optical records of the shock waves for supersonic jets and the jet boundary. For these studies a small convergent jet with an exit diameter of 1/8 in. was placed in the optical path of the interferometer. By using both beams of the interferometer, the density variations through the jet were obtained as indicated in Fig. 3 with the fringes parallel and perpendicular to the jet axis. For these optical data, the jet Mach number was approximately 1.4. Both white and green light sources were tried and it was found that the green light source gave better resolution of the diamond patterns for supersonic jets than the white light. When a convergent nozzle is operated with reservoir pressure greater than that for sonic Mach number at the exit, which is usually referred to as an underexpanded nozzle, shock bottles or diamond patterns[17,20] are formed due to the inertia effect of the gas. These shock patterns and the length of each bottle are more distinct with the fringes parallel to the jet axis as indicated in Fig. 3a, than with the fringes perpendicular to the jet axis, Fig. 3b. Approximately 7 shock bottles are visible with the ones located farthest downstream from the jet exit being very faint. With the fringes horizontal the supersonic jet boundary at the nozzle exit is very distinct and farther downstream the fringes have curvatures away from the jet axis indicating the spreading of the jet. In this photograph the shock bottles are visible but are not as well defined as those indicated in Fig. 3a.

Interferograms were obtained in Fig. 4 for a jet Mach number of 1.0 with the fringes parallel and perpendicular to the jet axis. Since the flow was sonic, there were no shock bottles present as observed in Fig. 3 for supersonic jet exhaust. But again with the fringes normal to the jet axis, Fig. 4b, the jet boundary is well defined in the immediate neighborhood of the jet exit and the curvature in the fringes farther downstream indicates the spreading of the subsonic jet. Interferograms for all other subsonic Mach numbers were quite similar to that observed for a jet Mach number of 1.0.

The schlieren photographs, Figs. 5 and 6, of the small jet were obtained by using one beam of the interferometer and placing a knife edge at the focal point. In these figures the schlieren photographs are for jet Mach numbers of 1.4 and 1.0. With the horizontal knife edge, Fig. 5a, the shock bottles are distinct close to the jet exit but farther downstream the shock waves are not as distinct because of the instability of the jet. Since the schlieren photographs

indicate the density gradient, the jet boundaries are clearly defined as the jet issues from the convergent nozzle. At a jet Mach number of 1.4 the amount of jet expansion from the nozzle exit is not very appreciable. Approximately 7 shock diamonds are visible with the shocks becoming faint towards the tip of the supersonic region. These shock patterns were practically identical to those observed with a 2 in. diameter convergent jet discussed in Ref. 23. For the sonic Mach number the schlieren photographs in Fig. 6 indicate only the outer edge of the jet boundary and the core region where there is large density gradient and no disturbance is present in the jet. Similar schlieren photographs were obtained for all subsonic jet Mach numbers. The shock waves in the supersonic jets and the jet boundary are more sharply defined in schlieren photographs than in the interferograms, Figs. 3 and 4, but the interferograms do indicate the spreading of the jet into the ambient air much more clearly from the curvature of the fringes.

Shadowgraphs of the subsonic and supersonic jet velocities, Fig. 7, were obtained by using the one beam of the interferometer without the knife edge. For the supersonic jet velocity, Fig. 7a, the strong shock waves in the initial shock bottles are very well defined because the shadowgraph photographs indicate the second derivative of the density gradient. In the photograph of the supersonic jet of Mach number 1.4, only 4 shock bottles are evident. The outer edge of the jet boundary is quite clearly defined at the nozzle exit for both sonic, Fig. 7b, and supersonic jet velocities. Thus, by using interferometer, schlieren, and shadowgraph photographs of jet at subsonic and supersonic velocities, it is possible to determine the location of the shock waves, large density gradient in the jet boundary, the core region, and the mixing of the jet with ambient gas.

3.1.2 Axial Velocity Distribution

The axial variations of the flow velocity along the jet axis were obtained by means of impact pressure and total temperature probes mounted on the trolley system, cf. Fig. 1, and moved from the jet exit to 80 in. downstream. With the convergent nozzle the jet expands from the exit for pressure ratios greater than the critical value. At supersonic jet velocities, the Mach number at the convergent nozzle exit is sonic as indicated in Fig. 8 and the static pressure is greater than the ambient pressure. Thus, in this figure the Mach numbers determined from the ratio of ambient to the impact pressure and the ratio of impact to the reservoir pressure are presented. These Mach numbers are given by the following equations:

$$\frac{p_a}{p_o'} = \left(\frac{2\gamma}{\gamma + 1} M^2 - \frac{\gamma - 1}{\gamma + 1}\right)^{\frac{1}{\gamma - 1}} \left(\frac{\gamma + 1}{2} M^2\right)^{-\frac{\gamma}{\gamma - 1}} \qquad [1]$$

and

$$\frac{p_o'}{p_o} = \left(\frac{(\gamma + 1)\, M^2}{(\gamma - 1)\, M^2 + 2} \right)^{\frac{\gamma}{\gamma - 1}} \left(\frac{\gamma + 1}{2\gamma\, M^2 - (\gamma - 1)} \right)^{\frac{1}{\gamma - 1}} \quad [2]$$

In the immediate vicinity of the convergent nozzle exit the Mach number determined from the ratio of the impact to the reservoir pressure is valid for supersonic jets in the core region. But farther downstream the primary jet mixes with the ambient gas so that the total energy of the jet is not equal to that in the reservoir. For these conditions the static pressure in the jet approaches the ambient pressure and consequently the Rayleigh formula, Eq. (1), should be more applicable to determine the local flow Mach number. In Fig. 8 for a jet Mach number of 1.4, the flow Mach numbers determined by these methods do agree at a distance of 10 in. from the nozzle exit. As the supersonic jet Mach number approaches unity, the difference between the Mach numbers determined by Eqs. (1) and (2) becomes smaller as indicated in Fig. 8 for a jet Mach number of 1.2.

The axial flow Mach numbers were determined by the ratio of ambient to impact pressure for all subsonic jet Mach numbers, including sonic. Over the jet exit Mach number range of 0.60 to 1.0, the axial variations of the velocity with distance were quite similar. For these subsonic jet Mach numbers the flow velocity was nearly constant over the initial 10 in. from the jet exit. This would indicate that the core region extended over 5 diameters from the convergent nozzle with an exit diameter of 2 in.

To determine the local flow velocity in the jet, both impact pressure and total temperature were measured separately on the jet axis. The relationship between the total temperature of the flow and the ambient temperature is given by

$$\frac{T}{T_o} = \left(1 + \frac{\gamma - 1}{2} M^2\right)^{-1} \quad [3]$$

Thus, knowing the flow Mach number from Eqs. (1) or (2) and the total temperature, the local ambient temperature was calculated from this equation. By assuming a perfect gas, the local velocity of sound was calculated from

$$c^2 = \gamma RT \quad [4]$$

and the local flow velocity by

$$v = M\,c \qquad [5]$$

The flow velocities determined by this method for various jet Mach numbers are presented in Fig. 9. For subsonic jet Mach numbers, the uniform velocity region extends to approximately 5 diameters before the flow velocity decreases with distance. The optical photographs presented in Figs. 4, 6 and 7 indicate the core region for subsonic jet Mach numbers and this correlates with the core region determined from the axial impact pressure and total temperature measurements. The velocity decay in the turbulent mixing region downstream of the core region is quite similar for all of the subsonic jet Mach numbers and agrees with the results presented in Ref. 16. For supersonic jet exit Mach numbers of 1.2 and 1.4, the sonic locations on the axis from Fig. 8 were 19.6 and 27.4 in. respectively. Using these distances in Fig. 9 to locate the sonic point, the flow velocity decay for both supersonic jet Mach numbers in the subsonic region is quite similar to that observed for subsonic jet exhaust velocities. Thus, for supersonic jet velocities, the location of the sonic point moves downstream with the supersonic Mach numbers, but the velocity decay in the subsonic turbulent region is similar to that observed for subsonic jets.

3.1.3 Jet Core Region and Supersonic Length

From the distributions of the Mach number and the flow velocity along the axis, Figs. 8 and 9, the jet core length, ℓ_c, and supersonic length, ℓ_s, were determined over the Mach number range of 0.60 to 1.40 from convergent nozzle. The core length is defined as the distance from the jet exit where the velocity on the axis is equal to that at the jet exit. Schlieren photographs in Fig. 6 for sonic velocity indicate the mixing of the jet with the ambient air as well as the core region. For subsonic Mach numbers the core length is approximately 5 diameters as indicated in Fig. 10. With a convergent nozzle at pressure ratios greater than the critical values for supersonic Mach numbers, there is no uniform core region because of the shock bottles as indicated in the Figs. 3, 5 and 7. This is not the case with a contoured nozzle operated at the design pressure ratio where the velocity from the nozzle exit is uniform and parallel with static pressure equal to the ambient pressure as discussed in Refs. 15 - 18. At sonic exit velocity the core and supersonic lengths were identical with the convergent nozzle. The supersonic region increased very rapidly with Mach number as indicated in Fig. 10. For supersonic Mach numbers the length of the supersonic region can be approximated by:

$$L_s = -32.50 + 48.75\ M_j - 11.25\ M_j^2 \qquad [6]$$

for the present convergent nozzle data. In Ref. 21 the available experimental data on the core and supersonic lengths for different types and sizes of nozzles and for various total temperatures were correlated, and the equations for the core and supersonic lengths were derived. By using the same pressure ratio and throat diameter for contoured and convergent nozzles, the supersonic length for the convergent nozzle was greater than for the contoured nozzle because of the shock bottles with corresponding less efficient mixing with the ambient air as discussed in Ref. 23.

3.1.4 Axial Impact Pressure Fluctuations

A small 1/4 in. diameter quartz piezoelectric pressure transducer with response time of approximately 20 microseconds was used to measure the impact pressure fluctuations along the axis for various jet Mach numbers. The rms values of the pressure fluctuations were obtained over an axial distance of 80 in. from the jet exit by the use of the moveable trolley, and are presented in Fig. 11. Over the subsonic Mach number range of 0.60 to 1.0, the variations of the impact pressure fluctuations with distance were quite similar with the peak fluctuations occurring at approximately 9 diameters from the jet exit. For subsonic Mach numbers, in the initial core region of approximately 5 diameters the pressure fluctuations are quite small compared to the peak value. From the optical results, Figs. 3 - 7, and the axial velocity distributions, it appears that the peak impact pressure fluctuations occur in the region where the primary jet is completely mixed with the surrounding gas. This region would correspond to the adjustment region as defined by Lighthill[1,2]. After this region the jet decays as a fully established turbulent jet flow and the impact pressure fluctuations decay monotonically. The decay in the impact pressure fluctuations beyond the peak value and in the axial velocity are quite similar for the subsonic jet Mach number range of 0.60 to 1.00.

As the jet velocity was increased to supersonic Mach numbers, the peak impact pressure fluctuations became greater than those observed for subsonic jets, cf. Fig. 11, and the location of the peak fluctuations was in the vicinity of the sonic velocity on the axis. At a jet Mach number of 1.4 the peak pressure fluctuations occurred just ahead of the sonic velocity on the axis while for a jet Mach number of 1.2 the location of the peak impact pressure was at the sonic point. The optical photographs of the Mach 1.4 jet, Figs. 3, 5 and 7, show the presence of large number of shock bottles, but evidently the impact pressure fluctuations at the normal shock waves in the bottles are not large compared to the fluctuations present at the end of the supersonic flow region.

At this Mach number the impact pressure should be the highest at the jet exit but the impact pressure fluctuations were quite small compared to the peak value. After the location of the peak fluctuations for supersonic jet Mach numbers, the fluctuations and the mean velocity, Fig. 9, decreased continuously like the subsonic jets. Thus, the maximum impact pressure fluctuations for supersonic jets occur in the vicinity of the sonic velocity on the jet axis while for subsonic jets the peak fluctuations occurred in the "adjustment region" of the jet.

3.2 Acoustic Characteristics of Subsonic and Supersonic Jets

3.2.1 Directivity of Far-Field Sound

The overall sound pressure levels were determined from the microphone measurements on a 10-ft. radius from the jet exit as shown in Figs. 1 and 2. Eight angular positions from the jet axis of 19.1° to 146.4° were used to determine the overall sound pressure levels, and the results for jet Mach numbers of 0.60 to 1.40 are presented in Fig. 12. For subsonic jet velocities the variations of the overall sound pressure level with angular position were quite similar with the maximum pressure level at an angular position of 19.1° and the pressure monotonically decreased with increasing angle. With room temperature subsonic jets, similar variations of the overall sound pressure level with angular position were observed by other investigators[3,6,7]. In Refs. 5 - 7 it was found that the directional characteristics of the sound field consisted of apparent sound sources for low and high frequencies. The angle of maximum intensity decreased with frequency, indicating the directivity distributions and the spectra of high and low frequencies are different with smooth transition between them.

Lassiter and Hubbard[3,4] had investigated the acoustic field distribution for subsonic jet exit velocities with a heated jet as well as with room temperature helium[3] as the working fluid. In both cases the exit velocities were supersonic relative to the ambient velocity of sound. With the helium the Mach number relative to the velocity of sound in air was approximately 2.8 even though the helium exit Mach number was 0.90. Under these subsonic jet exit Mach number conditions, the maximum overall sound pressure level was located at approximately 40° from the jet axis, which is located farther away from the jet axis than that observed for subsonic jets with room temperature air as shown in Fig. 12. These results indicate that both jet exhaust Mach number and the jet Mach number relative to the ambient velocity of sound are the parameters which determine the far field sound directivity pattern.

For supersonic jet Mach numbers the far field directivity patterns are different from those observed for subsonic jets as shown in Fig. 12. The maximum overall sound pressure levels were located close to the jet axis for supersonic Mach numbers and decreased to 43.8° location. Beyond this angular position the sound intensity remained nearly constant for the jet Mach number of 1.4. This type of sound pressure level variation is due to the occurrence of eight shock bottles at this Mach number with corresponding large acoustic radiation from each bottle as discussed in Ref. 20. When the supersonic jet is perfectly expanded through a contoured nozzle to the ambient air, there are no shock bottles as shown in Refs. 15 - 18. In Ref. 23 it was observed that the overall sound power level decreased with the angular position from the jet axis. In this reference, convergent and contoured nozzles were investigated with the same throat diameter and pressure ratio for a jet Mach number of 1.5. The comparison of the overall sound pressure levels in Fig. 12 indicates the difference in the variations with angular position for subsonic and supersonic jet Mach numbers from a convergent nozzle.

3.2.2 Sound Power Spectra

From the microphone measurements at eight angular positions, the spectra of the acoustic power output of the jet per 1/3 octave frequency band for jet Mach number range of 0.60 to 1.40 is shown in Fig. 13. With the available tape recorder the power spectra was obtained over a frequency range of 40 Hz to 16 kHz. There is appreciable scatter at frequencies below approximately 100 Hz. For these lower frequencies the wave length is becoming greater than the 10-ft. radius for the microphone and consequently the acoustic data will be in the near field at these lower frequencies, which causes the scatter as well as increasing the apparent acoustic power output. Gerrard[5] had obtained the power spectra for a small jet at room temperature over a Mach number range of 0.316 to 1.0 and obtained the spectra over a frequency range of approximately 150 Hz to 9 kHz. Over this frequency range the spectra presented in Fig. 13 are quite similar to that presented in Ref. 5. Over a jet Mach number range of 0.60 to 1.20 there appears a dip in the power spectra at approximately 4000 Hz in Fig. 13. Since other investigators[3-7] with subsonic jets have not obtained the dip in the power spectra at this frequency, it is very possible that the discontinuity in the power spectra was caused by the particular sound analyzer used in the present investigation.

For subsonic jet Mach numbers there is no noticeable change in the frequency of maximum power as indicated in Fig. 13. This same type of spectra was observed by Gerrard for subsonic jets. Even at a supersonic jet Mach number of 1.2 the power spectrum is very similar to that observed for the subsonic jets. At the

highest jet Mach number of 1.4 with the convergent nozzle, the maximum power occurred at higher frequency than that for the subsonic jets. Also, for this Mach number the discontinuity in the spectrum was not present. Acoustic data for the jet Mach number of 1.4 was obtained also with a tape recorder with response up to 80 kHz and the power spectrum from this data agreed with that observed with the tape recorder over a frequency range of 40 Hz to 16 kHz. For frequencies greater than 16 kHz the power continuously decreased indicating that nearly all of the acoustic power is contained in frequencies below 16 kHz for the 2 in. diameter nozzle. The Strouhal number for the frequency of 5 kHz for the peak power at a Mach number of 1.4 is 0.64. Comparison of sound power spectra in Fig. 13 between subsonic and supersonic jets indicates that the change in the power spectrum from subsonic to supersonic jet velocities is rather gradual and not as drastic as the overall sound pressure level shown in Fig. 12.

3.2.3 Overall Sound Power Level

The overall acoustic power output was calculated from the microphone data obtained at eight angular positions for each jet Mach number by

$$W = \frac{2\pi r^2}{\rho_a c_a} \int_0^{\pi} \bar{p}^2 \sin\theta \, d\theta \qquad [7]$$

where $\bar{p}$ is the rms sound pressure on the surface of a sphere of radius r, which is 10 ft., from the exit of the convergent jet. And the corresponding overall sound power level in db is given by

$$L_w = 10 \log_{10} \frac{W}{W_0} \qquad [8]$$

where W_0 is taken to be 10^{-13} watts. Overall sound power level as a function of the reservoir pressure for the convergent jet is presented in Fig. 14. The Mach number range corresponding to the reservoir pressures is 0.60 to 1.40. Sonic jet Mach number corresponds to a reservoir pressure of 13.1 psig. At the lower subsonic Mach numbers the overall sound power level increases rather steeply with jet Mach number and the slope decreases appreciably for supersonic jet Mach numbers. Since the total temperature was close to room temperature for these jet Mach numbers, the velocity, density, and temperature of the jet are not constant but are functions of the jet Mach number. Further discussion of the overall sound power levels will be made in a later section of this report.

3.2.4 Near Field Pressure Fluctuations

By using the trolley system, Figs. 1 and 2, and locating the microphone at various radial distances from the convergent nozzle exit, the variations in the near field pressure fluctuations with axial distance from the jet exit were determined for jet Mach numbers of 0.60 to 1.40 and are presented in Figs. 15a - e. The microphones were placed at radial locations of 2 to 8 nozzle diameters from the periphery of convergent nozzle exit, cf. Fig. 2. For subsonic jet Mach numbers of 0.60 to 1.0 the variations of the sound pressure level with axial distance for a given radial location were quite similar indicating the same type of acoustic radiation from subsonic jets, as well as for a sonic jet. The greatest increase in the sound pressure fluctuations with axial distance occurred with the microphone at the 2 diameter location. And the least variation of the sound pressure level with distance occurred with microphone eight diameters away from the nozzle for the subsonic Mach numbers.

From the axial impact pressure survey for these Mach numbers, it is noted that the uniform core region extends to 10 in. or 5 diameters as indicated in Figs. 8 and 9. But the near field sound pressure increased with distance beyond the core region for subsonic jet Mach numbers. This is reasonable because the sound pressure level at a particular radial and axial distances is influenced by the acoustic radiation from the upstream and downstream portion of the jet for subsonic exhaust velocities. And hence, the near field pressure level should increase with distance over the initial region from the jet exit as shown in Figs. 15a - c. At the jet exit the sound pressure levels at 3 and 4 nozzle diameters away from the jet were quite close but at larger axial distances the difference in the sound pressure levels became greater for all of the subsonic Mach numbers.

The variations of the near field sound pressure levels with radial and axial distances from the jet exit are presented in Figs. 15d - e for supersonic jet Mach numbers of 1.20 and 1.40. At all radial distances the sound pressure level variation with axial distances are very different than those observed for the subsonic jets, Figs. 15a - c. Again the largest pressure fluctuations were observed at a radial location of 2 diameters from the jet exit, but the variations in the sound pressure with distance were much less than those observed for the subsonic jets at the same radial location for the microphone. Also, for the radial location of 2 diameters there was greater local variations in the sound pressure levels for the subsonic jets. These local variations in the sound pressure level are probably due primarily to the Mach waves that are present for the convergent nozzle operated with choked throat as indicated in Refs. 17 and 20. Each shock bottle, cf. Figs. 3, 5 and 7, for supersonic jets is a source of strong acoustic radiation, including Mach waves.

The sound pressure levels at radial positions of 3 and 4 diameters are quite close with very little increase with axial distance. This was not the case for subsonic Mach numbers as indicated in Figs. 15a - c. The small decrease in the sound pressures over a radial distance of 3 to 4 diameters and very small increase with axial distance indicate that for supersonic jet Mach numbers the Mach waves are dominating the acoustic radiation from the jet in the vicinity of the nozzle exit. The attenuation of Mach waves with radial distance is much less than that for acoustic waves as observed for subsonic jets. The near field sound pressure level variation for a jet Mach number of 1.2 indicates the same type of acoustic radiation as observed for the jet Mach number of 1.4. This acoustic behavior is different from that postulated by various authors[1,24,25] for the turbulent eddy convective velocities for supersonic jets. They have assumed that the eddy convective velocity was approximately 0.6 of the jet velocity. For a jet Mach number of 1.2, this would correspond to subsonic Mach number of approximately 0.72 and for this convective Mach number there should be no Mach waves and this jet should be similar to a subsonic jet. But the present experimental results for the near field pressure measurements for a jet Mach number of 1.2 do not confirm this hypothesis. These near field pressure measurements indicate the distinct differences in the acoustic radiation from subsonic and supersonic jets as shown by Figs. 15 and 16 and Figs. 17 and 18. It is interesting that the near field sound pressures for a jet Mach number of unity are similar to those observed for subsonic Mach numbers.

Lassiter and Hubbard[4] had conducted similar experiments to determine the near field sound pressure levels from a one in. diameter jet with total temperature of 1660°R. The distribution of the sound pressures along the jet was obtained for four radial distances of .5 to 4.25 of the jet diameter at an exhaust velocity of 1240 fps, which corresponds to a jet Mach number of .64 and Mach number relative to ambient velocity of sound of 1.13. Under these conditions the location of the peak pressure fluctuations moved downstream from 4 diameters for a radial distance of .5 diameter to approximately 12 diameters for a radial distance of 4.25 diameters. These results are similar to those observed for the room temperature jet at a Mach number of 1.2 presented in Fig. 15d and do not agree with the results for the subsonic jet Mach number of 0.60, Fig. 15a. It is evident from these correlations with Lassiter and Hubbard data that the jet Mach number relative to the ambient velocity of sound is important for hot jets, where the jet Mach number can be subsonic but it is supersonic relative to the ambient gas.

Lassiter and Hubbard[4] also investigated the effects of the jet velocity on the sound pressure variation with axial distance at a radial distance of 2 diameters from the nozzle exit. With

a total temperature of 1660°R, the jet velocity was varied from 600 ft/sec. to 1870 ft/sec. and the corresponding jet Mach number varied from 0.31 to .96 while the Mach number relative to the ambient velocity of sound varied from 0.55 to 1.70. At the lowest velocity of 600 ft/sec. the overall sound pressure fluctuations remained nearly constant over the initial 6 diameters downstream of the jet exit before decreasing with distance. For this velocity the jet Mach numbers are subsonic and hence, one would expect that the pressure variation with distance should be similar to that observed for jet Mach number of 0.60, Fig. 15a. But the observed sound pressure variations do not agree and this difference may be caused by the difference in the total temperatures of 520° and 1660°R. Additional investigations must be conducted to resolve these results.

As the jet velocity was increased to 1870 ft/sec. the location of the peak sound pressure moved downstream to approximately 10 diameters, and the overall sound pressure continuously increased from the jet exit to the peak value before decreasing with distance. For this velocity the jet Mach number was 0.96 and the Mach number relative to ambient air was 1.70. The corresponding jet Mach numbers with room temperature jet would be approximately sonic, Fig. 15c, and 1.4, Fig. 15e. Comparisons of these figures with the data of Lassiter and Hubbard indicate that jet Mach number and the Mach number with respect to the ambient gas are important in the near field sound pressure distribution. The jet Mach number determines the length of the core and supersonic regions as indicated in Fig. 10 while the acoustic radiation from the jet is influenced by the jet Mach number relative to ambient velocity of sound. Further investigations must be conducted to obtain additional knowledge regarding the influence of jet Mach number, total temperature, and different gases upon the near field sound pressure distribution.

To show the differences in the near field sound pressure distributions for subsonic and supersonic jet Mach numbers more clearly, the sound pressure results presented in Fig. 15 for constant Mach numbers have been replotted in Fig. 16a and b for radial distances of 2 and 4 diameters and various jet Mach numbers. At a radial distance of 2 diameters, Fig. 16a, the variations of the sound pressure distributions with axial distance are similar for subsonic Mach numbers of 0.60 to 1.0 with the overall sound pressure level monotonically increasing with the axial distance. But for the supersonic jet Mach numbers of 1.2 and 1.4, the sound pressure levels at the jet exit location increased appreciably from that of jet Mach number of unity, and the increase in the sound pressure levels with distance was not as large as that observed for the subsonic jets. This difference in the near field pressure distributions are caused primarily by the appearance of the Mach waves for supersonic jets as discussed previously. Similar differences in the variation of the sound pressure distributions are still appreciable for radial location

of 4 diameters as shown in Fig. 16b. At this radial position the increase in the sound pressure level with axial distance for both subsonic and supersonic jets is not as great as that observed closer to the jet at 2 diameters.

In Fig. 16c the near field sound pressure distributions are presented for radial positions of 2 and 4 diameters and Mach numbers of 0.60 to 1.40. For subsonic Mach numbers of 0.60 to 1.0 the sound pressure distributions are similar for both radial positions of 2 and 4 diameters. But for supersonic Mach numbers of 1.2 and 1.4, the variations of the sound pressure level with distance are quite different from those of the subsonic jets at both radial positions of 2 and 4 diameters. Also, the attenuation of the sound pressure with radial distance is greater for the jet Mach number of 1.2 than 1.4. This may be due to the weaker waves present for the lower supersonic Mach number. The locations of the sonic velocity on the jet axis are also presented in this figure. In the subsonic region of the supersonic jets the attenuation in the sound pressures between the radial positions of 2 and 4 diameters is quite similar to that observed for subsonic jets.

4.0 CORRELATION WITH JET NOISE THEORIES

4.1 Jet Noise Theories

4.1.1 Subsonic Jet Noise Theory of Lighthill

Lighthill in Ref. 2 derived an equation for the overall sound power for subsonic jets based upon dimensional analysis and experimental acoustic data as

$$W = 10^{-4} \frac{1}{2} \rho_a \frac{U_j^8 A}{C_a^5} \qquad [9]$$

and assumed that the jet density ρ_j equals the ambient density ρ_a. To account for the differences in the physical state of the jet with that of the ambient gas, Eq. [9] can be expressed as

$$W = 10^{-4} \frac{m}{2} \frac{\rho_j}{\rho_a} \left(\frac{C_j}{C_a} \right)^5 C_j^2 M_j^7 \qquad [9a]$$

where $m = \rho_j U_j A$ is the mass flow of the jet. By assuming the sound emitted from the mixing region, $0 \leq x \leq 4D$, to be constant and the fully developed turbulent decay region as $4D \leq x < \infty$, the overall acoustic power output can be expressed as suggested by Lighthill by

$$W = \int_0^{4D} w_m \, dx + \int_{4D}^{\infty} w_m \, (4D)^6 \, x^{-6} \, dx \qquad [10]$$

where w_m is the sound emission per unit length in the mixing region. As shown in Ref. 21 the acoustic power output per unit diameter length in the mixing and turbulent decay regions can be expressed as

$$w_{d_m} = \frac{10^{-4}}{9.6} \frac{\rho_j}{\rho_a} m \left(\frac{C_j}{C_a} \right)^5 C_j^2 M_j^7, \quad 0 \leq x/D \leq 4 \qquad [11]$$

and

$$w_d = \frac{10^{-4}}{9.6\ (4^{-6})} \frac{\rho_j}{\rho_a} m \left(\frac{C_j}{C_a}\right)^5 C_j^{\,2} M_j^{\,7} \left(\frac{x}{D}\right)^{-6}, \quad 4 \leq x/D < \infty \quad [12]$$

These equations for the sound emission from subsonic jets will be correlated with the acoustic measurements.

4.1.2 Supersonic Jet Noise Theory of Nagamatsu and Horvay

An analysis of the acoustic power output for fully expanded supersonic jets was made by Nagamatsu and Horvay by considering the experimental aerodynamic and acoustic characteristics in Ref. 21. From the available data for jets with various exit diameters and temperatures it was found that the supersonic core length and the length of the supersonic region were functions of the jet Mach number. Also, in the supersonic region the acoustic emission per unit length was found to vary almost linearly with distance by Potter and Jones[15] for a perfectly expanded jet at a Mach number of 2.49. Nagamatsu, Pettit and Sheer[23] observed with a piezoelectric pressure transducer that the peak impact pressure fluctuations on the axis for jet Mach number of 1.5 occurred just ahead of the sonic velocity location. The present investigation of the near field sound pressures for supersonic jets indicated that the sound pressure levels increased almost linearly from the jet exit to the sonic location as shown in Fig. 16c. From the sound pressure measurements made with microphones at 2 and 4 diameter locations, acoustic radiations per unit length for Mach numbers of 1.2 and 1.4 were calculated and are plotted in Figs. 17d, 17e, and 19b. These results indicate that the assumed linear variation of the sound emission per unit length of the jet is reasonable for a convergent nozzle operated at supersonic flow conditions.

Using the relationship for the supersonic length, the linear variation of the acoustic power radiation per unit length in the supersonic region and the subsonic turbulent decay, x^{-6}, an equation for the overall acoustic power output for supersonic jets was derived by Nagamatsu and Horvay in Ref. 21. The overall sound power output from a supersonic jet can be expressed as a sum of the acoustic contribution from the supersonic region $0 \leq x \leq \ell_s$, and the subsonic turbulent decay region, $\ell_s \leq x < \infty$, by

$$W = \int_0^{\ell_s} w\, dx + \int_{\ell_s}^{\infty} w\, dx \quad [13]$$

where w is the acoustic power output of a jet slice of unit length and is a function of x for given jet conditions. This

may be written with $w_d = w\ D_j$ as

$$W = \int_0^{L_s} w_d\ d(x/D) + \int_{L_s}^{\infty} w_d\ d(x/D) \qquad [14]$$

It is shown in Ref. 21 that the acoustic power output per unit diameter length is given in the supersonic region, $0 \leq x/D \leq L_s$, by

$$w_d = \frac{10^{-4}}{9.6}\, m\, \frac{\rho_j}{\rho_a} \left(\frac{C_j}{C_a}\right)^5 \left(C_j^{\,2}\, M_j^{\,7-\alpha}\right) \left(1 + \frac{M^{\alpha-\beta} - 1}{5M_j^{\,2} + 0.8}\right) (x/D) \qquad [15]$$

and in the subsonic region, $L_s \leq x/D < \infty$, by

$$w_d = \frac{10^{-4}}{9.6}\, m\, \frac{\rho_j}{\rho_a} \left(\frac{C_j}{C_a}\right)^5 \left(C_j^{\,2}\, M_j^{\,7-\beta}\right) \left(5M_j^{\,2} + 0.8\right)^6 (x/D)^{-6} \qquad [16]$$

where α and β are exponents which must be evaluated from experimental acoustic data. Substituting Eqs. [15] and [16] into Eq. [14], the total acoustic power output from a supersonic jet is given by

$$W = \frac{10^{-4}}{9.6}\, m\, \frac{\rho_j}{\rho_a} \left(\frac{C_j}{C_a}\right)^5 \left(C_j^{\,2}\, M_j^{\,2}\right) \left(5M_j^{\,2} + 0.8\right) \left(\frac{M_j^{-\alpha} + M_j^{-\beta}}{2} + \frac{M_j^{-\beta}}{5}\right) \qquad [17]$$

These equations derived by Nagamatsu and Horvay were used to analyze the sound emission from supersonic jets. The supersonic jet noise analyses by Phillips[24] and Williams[25] do not take into consideration the observed aerodynamic and acoustic characteristics for supersonic jets.

4.2 Distribution of Acoustic Power Emission

By placing two microphones, one on each side of the jet, at various radial distances, the near field sound pressure variations with axial distance were determined over a range of Mach number of 0.60 to 1.40. Lassiter and Hubbard[4] had conducted similar experiments with a hot air jet and obtained interesting results as discussed previously in this report. From these sound pressure measurements in the near field, the acoustic intensity and the acoustic power transmitted through a cylindrical

surface were calculated to obtain information regarding the acoustic radiation characteristics for subsonic and supersonic jets.

The intensity of acoustic radiation at the microphone location is given by

$$I = \frac{\bar{p}^2}{\rho_a \, c_a} \qquad [18]$$

where $\bar{p}$ is the rms sound pressure. By assuming that the sound emission from the circular jet is axially symmetric, the sound power transmission per unit length through a cylindrical surface containing the microphone is

$$w = \int_0^{2\pi} \frac{\bar{p}^2}{\rho_a \, c_a} \, r \, d\theta \qquad [19]$$

and in terms of unit jet diameter length

$$w_d = \frac{D}{\rho_a \, c_a} \int_0^{2\pi} \bar{p}^2 \, r \, d\theta \qquad [19a]$$

Using these equations the acoustic power transmissions through the cylindrical surfaces were calculated and are presented in Figs. 17 - 19 for various radial distances and jet Mach numbers.

The acoustic power transmissions per unit length of the cylindrical surface concentric with the jet are presented in Figs. 17a - c for subsonic jet Mach numbers of 0.60, 0.85, and 1.0. At the lowest jet Mach number the acoustic power radiation is extremely small at the jet exit. With the microphone located at a radial distance of 2 diameters, the calculated acoustic power transmission increases very rapidly with axial distance. At this radial location the jet spreads out with distance and approaches the microphone. For all subsonic Mach numbers the uniform core extended to approximately 5 diameters. The acoustic power passing through a cylindrical surface with radius of 2 to 4 diameters decreases continuously with radial distance from the jet axis. At a radial distance of 8 diameters the acoustic power per unit length was nearly constant. Similar results were obtained for jet Mach numbers of 0.85 and 1.0 as indicated in Figs. 17b and c. For these subsonic Mach numbers the acoustic

power at the plane of the jet exit was very low and did not vary with the radial distance. Lighthill[1,2] in his analysis of subsonic jets assumed that the sound emission from the jet was constant over the mixing region of 4 diameters from the exit. These preliminary near field sound pressure measurements do not indicate this phenomenon, but additional investigations will be conducted to resolve this question. Downstream of the initial mixing region, which extends to approximately 5 diameters in the present investigation, Lighthill assumed a turbulent decay in the acoustic radiation as being proportional to x^{-6}. At the cylindrical surfaces determined by the microphone location, the acoustic power transmitted through the surface continuously increased for the subsonic jet Mach numbers, Fig. 17a - c. This observed result was due to the fact that the microphone measured the sound pressures contributed by the acoustic radiation from the regions of the jet upstream and downstream of the microphone axial position. For subsonic jet velocities the acoustic radiation from turbulence in the jet can reach the microphone placed in the near field by eddies that are downstream of the microphone.

The distributions of acoustic power transmission per unit length of cylindrical surface concentric with the jet are presented in Figs. 17d and e for supersonic jet Mach numbers of 1.2 and 1.4. The acoustic power distributions for these supersonic Mach numbers are quite different from those observed for the subsonic Mach numbers, Figs. 17a - c. At the jet exit plane, the acoustic powers are quite large for radial distances of 2 and 4 diameters. While for subsonic jet Mach numbers and Mach number of unity the acoustic power at this axial location was quite low and did not vary with the radial distances. The variation of the acoustic power transmission per unit length in the axial direction with microphone at radial position of 2 diameters is not continuous but can be approximated by a linear variation up to the sonic location as indicated in Figs. 17d and e. Even by increasing the Mach number from 1.0 to 1.2, there occurs a drastic change in the distribution of the acoustic emission from the jet. The decrease in the acoustic power for a change in radial distance of 3 to 4 diameters is small. These results for the supersonic jets indicate the existence of both Mach and acoustic waves as shown in Refs. 15, 17 and 20 for the sound emission from supersonic jets.

In Figs. 18a and b the distribution of the acoustic power propagation through cylindrical surfaces of 2 and 4 diameters from the nozzle exit are presented for jet Mach numbers of 0.60 to 1.4. For subsonic Mach numbers the acoustic power distributions are similar for both radial distances of 2 and 4 diameters with continuous increase in power with axial distance. The rate of increase of the acoustic power with distance is greater for the microphone located closer to the jet

periphery. For supersonic Mach numbers of 1.2 and 1.4 the acoustic power distributions with distance were drastically different from those observed for subsonic jet Mach numbers as indicated in Figs. 18a and b. The greatest change in the acoustic power occurred at the plane of the jet exit for both radial distances. Over the supersonic region of the jets the acoustic power distribution increased almost linearly with distance for a radial distance of 2 diameters and the rate of increase of the power with distance was much less than that observed for the subsonic jets. As mentioned previously this difference in the acoustic power distribution is due primarily to the presence of Mach waves for supersonic jets.

To obtain some information regarding the acoustic power radiation from a convergent nozzle, the acoustic power per unit exit diameter length for various Mach numbers were calculated and are presented in Figs. 19a and b for a radial distance of 2 diameters from the jet exit. In the uniform core region of 5 diameters for the subsonic jets the acoustic power distribution was approximated by a straight line as indicated in Fig. 19a, and it was assumed downstream of the core region that the acoustic power decreased as x^{-6} in the turbulent decay region. The acoustic power distributions presented in Fig. 19a were integrated to obtain the overall acoustic power level by

$$W = \int_0^{\ell_c} w\, 2\pi\, r\, dx + \int_{\ell_c}^{\infty} w\, 2\pi\, r\, \ell_c^{6}\, x^{-6}\, dx \qquad [20]$$

where $r = 2.5D$ and $\ell_c = 5D$ for jet Mach numbers of 0.85 and 1.0. The overall acoustic power levels calculated by this method for the near field measurements were 129 and 134 db for jet Mach numbers of 0.85 and 1.0 respectively. The corresponding overall power level determined from the microphone measurements on a radius of 10 ft. from the jet exit were 135 and 140 db respectively. Thus, the overall acoustic powers calculated from the near field measurements and assumed power distribution were approximately 6 db lower than that determined from the far field measurements. Further investigations will be conducted to determine the acoustic power emission from subsonic jets.

The overall acoustic power levels were also calculated for jet Mach numbers of 1.2 and 1.4 by the use of Eq. [20] with the supersonic length ℓ_s from the near field measurements and the results are presented in Fig. 19b. From these Mach numbers the acoustic power distribution was approximated by a straight line up to the sonic point as determined from Figs. 8 and 9. This linear approximation in the supersonic region

seems to be reasonable and it was used by Nagamatsu and Horvay[21] in developing the supersonic jet noise theory. Downstream of the supersonic region in the subsonic turbulent jet mixing region the acoustic power distribution was assumed to vary as x^{-6}, same variation as assumed by Lighthill[1,2] for subsonic jets. The scatter in the acoustic power distribution from the straight line for Mach 1.2 was much less than that observed for the Mach 1.4 because of the smaller number of shock bottles and weaker waves at the lower supersonic Mach number. The overall acoustic power levels calculated by Eq. [20] for jet Mach numbers of 1.2 and 1.4 were 149 and 158 db respectively. From the microphone measurements on a 10-ft. radius, the corresponding far field overall acoustic power levels were 148 and 156 db respectively. These results indicate a surprising agreement between the overall acoustic power level determined from near field and far field measurements for supersonic jets. This excellent agreement may be due to two factors. Firstly, at these supersonic Mach numbers the sound power spectra, Fig. 13, indicate that the frequency for the peak power was approximately 5 kHz and the corresponding wave length of 0.22 ft. Thus, the microphone was located approximately 1.5 times the wave length from the jet periphery. The second factor is due to the existence of Mach waves for supersonic jets as shown in Refs. 15, 17 and 20. Thus, in the near field location the microphone will be influenced primarily by the Mach waves and sound waves from the region of the jet upstream of the microphone location. And the sound emission from the region of the jet downstream of the microphone will be highly attenuated or will not reach the microphone because of the supersonic jet velocity. Additional investigations will be conducted to determine the acoustic power distribution from supersonic jets, both from convergent and parallel flow nozzles.

The overall acoustic power levels determined from the near and far field microphone measurements are presented in Fig. 20 for jet Mach numbers of 0.60 to 1.4. For a jet Mach number of 1.4 the overall sound power levels determined from microphone measurements at radial distances of 2 and 4 diameters from the jet exit brackets the overall sound power level determined from far field measurements. Similar results were obtained for jet Mach number of 1.2 with the far field result being closer to that determined from a radial distance of 2 diameters. But at subsonic Mach numbers of 0.85 and 1.0, the overall sound power levels calculated from near field measurements were less than that determined on a 10-ft. radius from the jet exit. The overall sound power levels determined from the near and far field sound measurements agreed quite well for the subsonic jet Mach numbers of 0.60 and 0.70 for 2 diameters as indicated in Fig. 20. These preliminary results for the overall sound power levels indicate that for supersonic jets the near field acoustic measurements can be used to obtain the overall sound power radiation as well as the approximate acoustic power emission

distribution from the supersonic region of the jet. For subsonic jet Mach numbers close to sonic, the near field acoustic measurements give some indication of the overall sound power level and the distribution of the sound emission from the core region of the jet.

4.3 Evaluation of Exponents α and β and Overall Sound Power Level

The overall sound power levels for a 2 in. diameter convergent nozzle with unheated air are presented in Fig. 21 over a jet Mach number range of 0.60 to 1.4. This same data was plotted in Fig. 14 as a function of the reservoir pressure. Since the overall sound power depends upon the mass of the jet for constant reservoir conditions as shown by Eqs. 9 and 17, the experimental sound power levels in Fig. 21 are corrected to unit slug mass per second for each jet Mach number.

For these experimental test conditions the overall sound power levels were calculated by the use of Lighthill's subsonic jet noise theory[1,2] given by Eq. 9a in this report, with the assumption that the density of the jet equal to the ambient density, and also with the actual jet and ambient densities. At subsonic Mach numbers the correction for this jet density effect is small and the correction increases with Mach number. For the lowest subsonic Mach number of 0.60, the overall sound power level predicted by Lighthill's theory agrees with the observed experimental value. Also, the core region for the subsonic Mach numbers extended approximately over 5 diameters as shown in Figs. 8 and 9 and Lighthill assumed this to be 4 diameters. But for higher Mach numbers the agreement of Lighthill's prediction with the experimental data becomes poorer and at a Mach number of 1.4 the difference was approximately 8 dbs. Thus, the correlation of Lighthill's predictions with the experimental acoustic data for unheated air jet indicates that Lighthill's theory can be used for subsonic jets, but for supersonic jets the theory does not apply because the acoustic model used in deriving the overall sound power level does not agree with the supersonic jet characteristics. It has been found experimentally that the peak acoustic power is generated close to the end of the supersonic region for supersonic jets[15,23] and this location is much greater than 4 diameters assumed by Lighthill. It was also observed that the acoustic power emission is not constant in the supersonic region. These are characteristics of supersonic jets which are different than the flow and acoustic models assumed by Lighthill in his analysis for subsonic jets.

As a first approximation the values of the exponents α and β in the supersonic jet noise theory of Nagamatsu and Horvay[21], given by Eq. [17] in the present report, were determined from the acoustic distribution determined by Potter and Jones[15] for a parallel flow nozzle at a Mach number of 2.49. For this jet the values of α and β were 6.2 and 2.4 respectively.

Using these values in Eq. [17], the overall sound power levels were calculated and are presented in Fig. 21. At sonic jet Mach number the calculated value agreed with the experimental observation, but for supersonic Mach numbers the calculated values were less than the experimental data for the convergent nozzle. With these values for α and β, the length of the supersonic region determined from Eq. [17] was close to the observed length but these values did not predict the correct acoustic emission from the jet exit or at the sonic location. From the acoustic measurement at a Mach number of 1.4 the values of α and β were determined to be .356 and -1.17 respectively, cf. Fig. 22. Similarly the values of α and β were found to be .229 and -.962 for a jet Mach number of 1.2. These values of α and β for the supersonic Mach numbers agree with the acoustic power distributions given in Fig. 19b.

In Fig. 22 the values of the exponents α and β for the Nagamatsu and Horvay supersonic jet noise theory are presented as a function of the jet Mach number for convergent and parallel flow nozzles. Also, the function given by

$$F(M_j) = \frac{M_j^{-\alpha} + M_j^{-\beta}}{2} + \frac{M_j^{-\beta}}{5} \qquad [21]$$

from Eq. [17] is presented in this figure. A contoured nozzle[23] with a throat diameter of 2 in. and exit Mach number of 1.5 was used to determine the values of α and β. The values for a parallel nozzle with exit Mach number of 2.49 were determined from Ref. 15. Since the supersonic flow from a convergent nozzle contains shock bottles, Figs. 3, 5 and 7, while there is no such shock system for parallel flow nozzles, the values of the exponents α and β should depend upon the type of nozzle as indicated in Fig. 22. Also, the value of $F(M_j)$ is greater for the convergent nozzle than the parallel flow nozzle because of the existence of shock bottles with additional noise source as discussed by Dosanjh[20]. Additional experiments will be conducted to define the variation of α, β, and $F(M_j)$ with Mach number for different types of nozzle and at various total temperatures.

Recently, the overall sound power levels[23,26] of jets from different size converging nozzles at a Mach number of 1.4 were compared. The nozzles considered were a 2 in. diameter with unheated air, a 4.3 in. diameter at 2300°R, and approximately a 45 in. diameter GE4 engine at 2500°R. It was found that the values of the exponents α and β determined from the unheated 2 in. diameter jet agreed within experimental accuracy with the values determined from the 4.3 in. and 45 in. diameter jets at high temperatures. These

preliminary results indicate that for supersonic jets the Mach number is the important variable for the length of the supersonic region and the overall sound power level. The Reynolds number of the jet and the total temperature seem to be of secondary importance on the noise output.

Experimental and analytical values of the overall sound power level are presented in Fig. 23 as a function of the jet velocity. In this figure the theoretical curves were calculated from the supersonic jet noise theory of Nagamatsu and Horvay[21], Eq. [17]. The values of the exponents α and β in this equation were taken to be 6.2 and 2.4, which were evaluated from the acoustic data at a Mach number of 2.49 obtained by Potter and Jones for a parallel flow jet. The slope of the overall sound power level as a function of the velocity is dependent upon the total temperature of the jet which influences the ratio of the densities of the jet and ambient gas, ρ_j/ρ_a. This density ratio appears in the overall sound power level given by Eq. [17]. The dashed portion of the acoustic power level curves for each jet total temperature is for subsonic jet velocities. Both the acoustic data obtained by Tatge and Wells[27] for a heated air jet and in the present investigation were corrected to unit slug mass for the jet by Eq. [17] in order to correlate with the theoretical predictions. The present acoustic data were for a convergent nozzle with an exit diameter of 2 in. and the results are shown in Fig. 23 for a Mach number range of 0.85 to 1.40 at a total temperature of 538°R. The slope of the experimental curve is steeper than the calculated curve for a total temperature of 520°R, and $\alpha = 6.2$ and $\beta = 2.4$. It was shown in Fig. 21 that the values for the exponents α and β are functions of the type of nozzle and the jet Mach number. With the values of the exponents presented in Fig. 22 for the convergent nozzle the overall acoustic power level will agree with the experimental data.

Acoustic characteristics of heated air from 4 in. diameter convergent nozzle were determined by Tatge and Wells[27] at a total temperature of 2000°R over a Mach number range of 0.89 to 1.47 and the results corrected to unit mass flow are presented in Fig. 23. For these experiments the nozzle was mounted 30 ft. above the ground and the jet discharged vertically to minimize the ground reflection effects on the acoustic measurements. The slope of the variation of the overall sound power level with the jet velocity is much less than that observed for the lower temperature of 538°R as indicated in Fig. 23. But the slope agrees approximately with the theoretical prediction given by Eq. [17]. If the values for α and β presented in Fig. 22 are used in Eq. [17] instead of $\alpha = 6.2$ and $\beta = 2.4$, better agreement between the experimental and theoretical results would be obtained for this total temperature condition.

The range of jet Mach number for the total temperature of 538°R was from 0.85 to 1.4 while the corresponding Mach

number range was from 0.89 to 1.4 for a total temperature of 2000°R. But for approximately the same Mach number range there was a large difference in the slope of the curves for the variation of the overall sound power level with jet velocity. It was shown in Ref. 21 that the length of the supersonic region for supersonic jets was primarily a function of the jet Mach number and that the jet total temperature and the Reynolds number were of secondary importance. The supersonic lengths for both total temperatures of 538° and 2000°R for the same supersonic Mach number would be approximately the same. Also, the exponential values for α and β would be approximately the same for a fixed supersonic jet Mach number as observed in Ref. 26. Thus, the decrease in the slope of the variation of the overall sound power level with jet velocity is due mainly to the decrease in the jet density as derived in the supersonic jet noise theory of Nagamatsu and Horvay. Additional carefully controlled experiments must be conducted at various elevated jet temperatures to obtain more information regarding the acoustic characteristics for supersonic jets.

5.0 CONCLUSIONS

Convergent and parallel flow nozzles with 2 in. diameter throats were used with a room temperature air supply to produce jet Mach numbers of 0.60 to 1.50. Both aerodynamic and acoustic measurements were made to determine the characteristics of subsonic and supersonic jets.

The axial distributions of Mach number, velocity, and temperature were determined for the convergent nozzle over a Mach number range of 0.60 to 1.4. For subsonic Mach numbers, including sonic Mach number, the velocity on the axis remained constant over a distance of approximately 5 diameters before decreasing in the turbulent decay region.

For a supersonic jet Mach number of 1.4 the sonic velocity occurred at 13.7 diameters from the jet exit and the length of the supersonic region was proportional to M_j^2. Downstream of the sonic point the velocity decay was similar to that observed for subsonic jets.

The impact pressure fluctuations on the jet axis were determined with a quartz piezoelectric pressure transducer. For subsonic jet Mach numbers the peak total pressure fluctuations occurred at approximately 9 diameters from the jet exit, but for a supersonic jet Mach number of 1.4, the peak pressure fluctuations occurred at approximately 12.5 diameters, just ahead of the sonic point.

The highest overall sound pressure levels occurred at an angular position of 19.1° from the jet axis for both subsonic and supersonic jets. For the subsonic jets the overall sound pressure levels decreased monotonically with the increase in the angular position from the jet axis. But for a supersonic jet Mach number of 1.4, the overall sound pressure level decreased over the angular positions of 19.1° to 43.8° and then remained nearly constant for larger angular positions.

Power spectra for subsonic jets were quite similar with the peak power occurring at approximately 4 kHz for Mach numbers of 0.60 to 1.0. At a jet Mach number of 1.4 the peak power occurred at a frequency of 5 kHz which corresponds to a Strouhal number of 0.64.

Near field sound pressure levels were determined with microphones placed 2 to 8 diameters away from the nozzle exit. The variations of the overall sound pressures with axial distance for a particular radial position of the microphone were quite similar for jet Mach numbers of 0.60 to 1.0. But for jet Mach numbers of 1.2 and 1.4 the sound pressure levels at the jet exit plane were much greater than that observed for a jet Mach number of unity and the variations of the sound

pressure levels with distance were quite different than those observed for subsonic jets. This difference in the sound pressure distributions may be due to the presence of Mach waves from supersonic jets.

From the near field pressure measurements the distributions of the acoustic power transmission through a cylindrical surface for a given radial location of the microphone were determined for both subsonic and supersonic jets, and were found to be quite different. For supersonic jet Mach numbers the acoustic power distribution increased almost linearly from the jet exit to the sonic velocity location. And by assuming the acoustic power decay as x^{-6} in the subsonic region, the overall sound power levels were determined and the values agreed closely with those observed in the far field.

Overall sound power levels for Mach numbers of 0.60 to 1.5 were determined and compared with the subsonic theory of Lighthill and the supersonic theory of Nagamatsu and Horvay. At a jet Mach number of 0.60 the aerodynamic flow model and the overall sound power level agreed with the prediction of Lighthill. But at higher Mach numbers the experimental overall sound power levels were higher than Lighthill's prediction and at a Mach number of 1.4 the measured sound power level was approximately 8 dbs higher than the prediction.

At supersonic jet Mach numbers the aerodynamic flow model and the acoustic power distribution agreed with the assumption used in the derivation of the Nagamatsu and Horvay jet noise theory. The exponents α and β in the theory were evaluated for convergent and parallel flow nozzles as functions of the jet Mach number. Overall sound power levels for jet Mach numbers of 0.60 to 1.4 were compared with the supersonic theory.

REFERENCES

1. Lighthill, M.J., The Bakerian Lecture, 1961, "Sound Generated Aerodynamically", Proc. Roy. Soc. A267, 147-182, (1962).

2. Lighthill, M.J., "Jet Noise", AIAA Jour., Vol. 1, No. 7, 1507-1517, (1963).

3. Lassiter, L.W. and Hubbard, H.H., "Experimental Studies of Noise from Subsonic Jets in Still Air", NACA TN 2757, (1952).

4. Lassiter, L.W. and Hubbard, H.H., "The Near Field Noise of Static Jets and Some Model Studies of Devices for Noise Reduction", NACA Rpt. 1261, (1954).

5. Gerrard, J.H., "An Investigation of the Noise Produced by Subsonic Air Jet", J. Aero. Sci., 23, 855-866, (1956).

6. Mollo-Christensen, E. and Narasimha, R., "Sound Emission from Jets at High Subsonic Velocity", J. Fluid Mech., 8, 49-60, (1960).

7. Mollo-Christensen, E., "Jet Noise and Shear Flow Instability Seen From an Experimenter's Viewpoint", Trans. of ASME, Paper No. 67, APM-C, (1966).

8. Laurence, J.C., "Intensity, Scale, and Spectra of Turbulence in Mixing Region of Free Subsonic Jet", NACA Rpt. 1292, (1956).

9. Davies, P.O.A.L., Fisher, M.J. and Barratt, M.J., "The Characteristics of the Turbulence in the Mixing Region of a Round Jet", J. Fluid Mech., 15, 337-367, (1963).

10. Chu, W.T., "Turbulence Measurements Relevant to Jet Noise", Inst. of Aerospace Sci., UTIAS Rpt. 119, (1966).

11. Davies, P.O.A.L., Ko, N.W.M. and Bose, B., "The Local Pressure Field of Turbulent Jets", Ministry of Technology, Aero. Res. Council, C.P. No. 989, (1967).

12. Jones, I.S.F., "Fluctuating Turbulent Stresses in the Noise-Producing Region of a Jet", J. Fluid Mech., 36, Part 3, 529-543, (1969).

13. Powell, A., "The Noise of Choked Jets", JASA, Vol. 25, 385-389, (1953).

14. Mayes, W.H., Lanford, W.E. and Hubbard, H.H., "Near Field and Far Field Noise Surveys of Solid Fuel Rocket Engines for a Range of Nozzle Exit Pressures", NASA TN D-21, (1959).

15. Potter, R.C. and Jones, J.H., "An Experiment to Locate the Acoustic Sources in a High Speed Jet Exhaust Stream", Wyle Lab. Rpt., (1967).

16. Warren, W.R., "An Analytical and Experimental Study of Compressible Free Jets", Doctoral Dissertation, Princeton Univ., (1957).

17. Love, E.S., Grigsby, C.E., Lee, L.P. and Woodling, M., "Experimental and Theoretical Studies of Axisymmetric Free Jets", NASA Rpt. TR-6, (1959).

18. Eggers, J.M., "Velocity Profiles and Eddy Viscosity Distribution Downstream of a Mach 2.2 Nozzle Exhausting in Quiescent Air", NASA TN D-3601, (1966).

19. Mayes, W.H., Philip, M.E., Jr. and James, S.O., Jr., "Near-Field and Far-Field Noise Measurements for a Blowdown-Wind-Tunnel Supersonic Exhaust Jet Having About 475,000 Pounds of Thrust", NASA TN D-517, (1961).

20. Dosanjh, D.S. and Montegani, F.J., "Reduction of Noise from Underexpanded Axisymmetric Jet Flows Using Radial Jet Flow Impingement", AIAA Paper No. 68-81, (1968).

21. Nagamatsu, H.T. and Horvay, G., "Supersonic Jet Noise", General Electric Res. and Dev. Ctr. Rept. 69-C-161, (1969).

22. Nagamatsu, H.T., Sheer, R.E., Jr. and Wells, R.J., "Supersonic Jet Exhaust Noise Reduction with Rods, Shroud, and Induced Flow", Proc. AFOSR-UTIAS Symposium on Aerodynamic Noise in Toronto, (1968).

23. Nagamatsu, H.T., Pettit, W.T. and Sheer, R.E., Jr., "Flow and Acoustic Measurements on a Convergent Nozzle Supersonic Jet Ejector", General Electric Res. and Dev. Ctr. Rept. 69-C-156, (1969).

24. Phillips, O.M., "On the Generation of Sound by Supersonic Turbulent Shear Layers", J. Fluid Mech., 9, Part 1, 1-28, (1960).

25. Williams, J.E.F., "The Noise from Turbulence Convected at High Speed", Phil. Trans. Roy. Soc., London, Series A, 255, 479-503, (1963).

26. Private Communication from C.Y. Chen, (1969).

27. Tatge, R.B. and Wells, R.J., "Model Jet Noise Study at Alplaus Facility", General Electric Engineering Laboratory Rept. 61GL25, (1961).

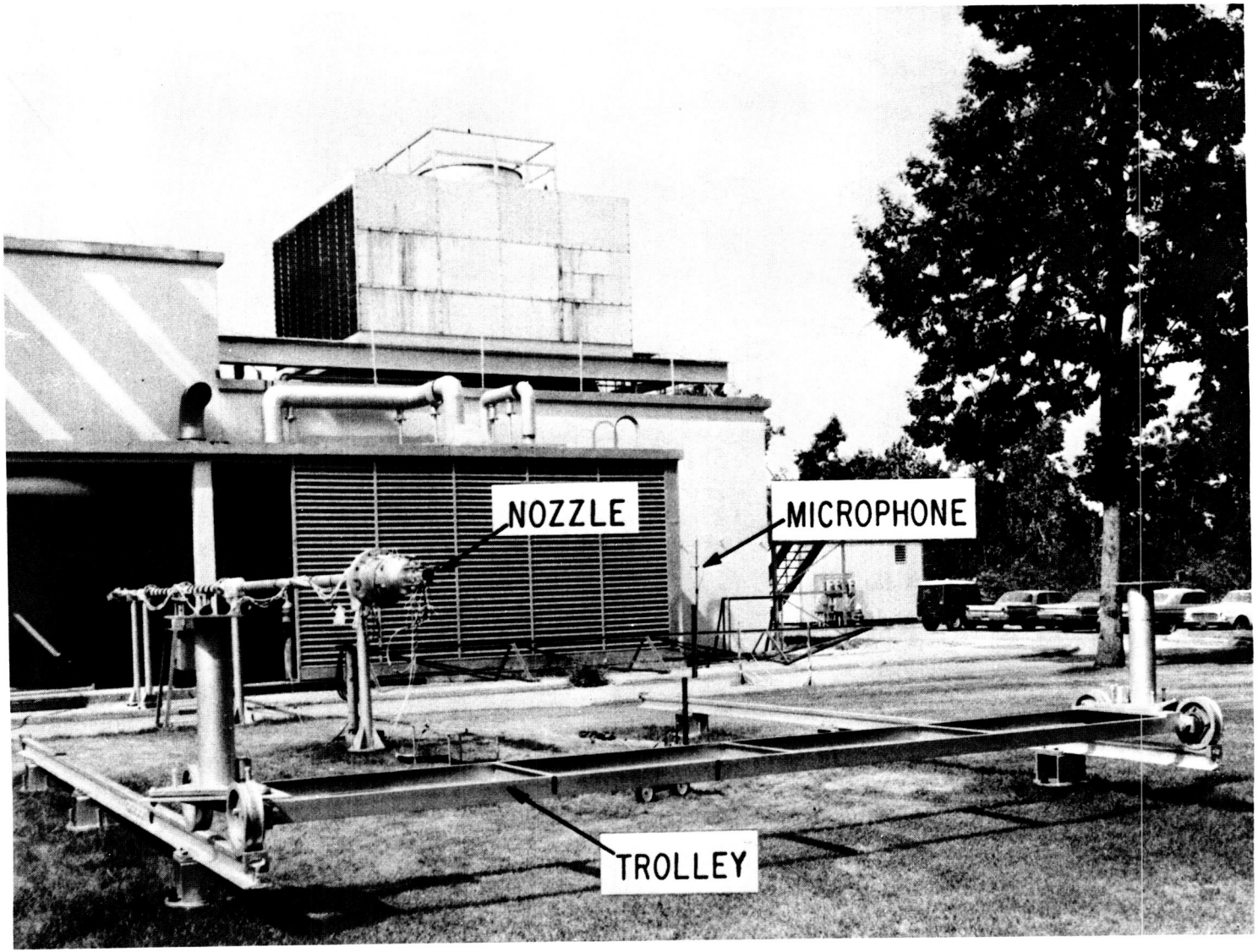

FIG. 1. PHOTOGRAPH OF GENERAL ELECTRIC RESEARCH AND DEVELOPMENT CENTER SUPERSONIC JET EXHAUST TEST FACILITY.

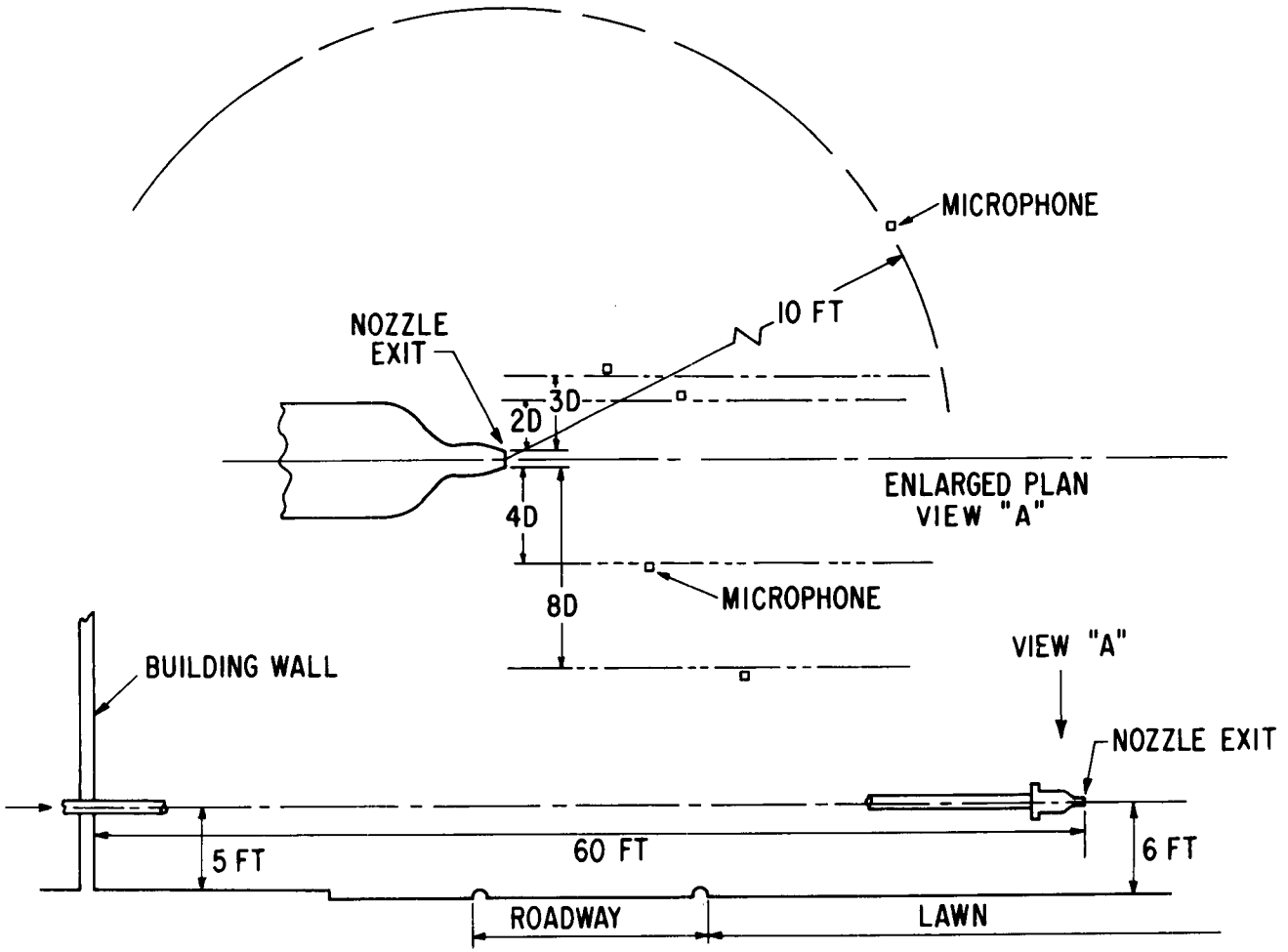

FIG. 2 SCHEMATIC OF SUPERSONIC JET NOISE TEST FACILITY.

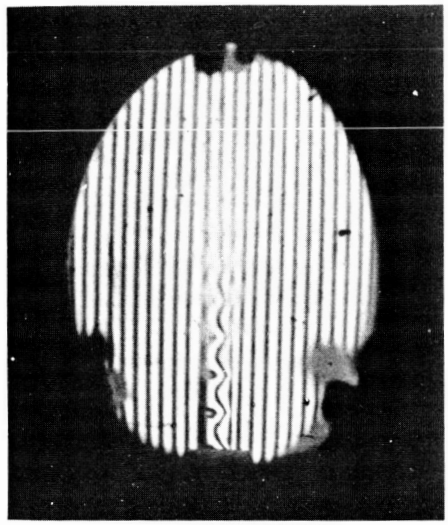

3(a)

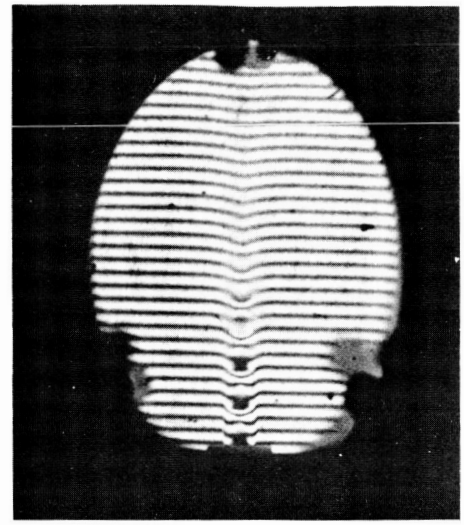

3(b)

FIG. 3 INTERFEROMETER PHOTOGRAPHS OF FLOW FROM A CONVERGENT NOZZLE AT MACH NUMBER OF 1.4

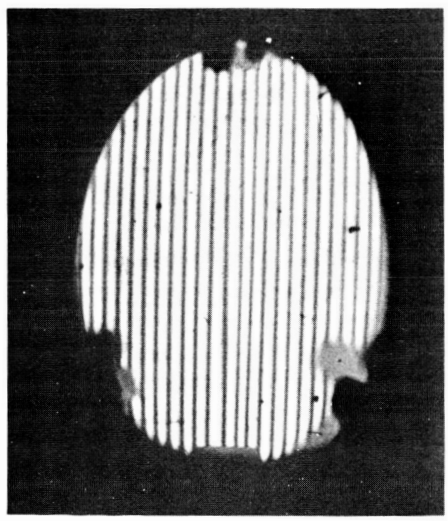

4(a)

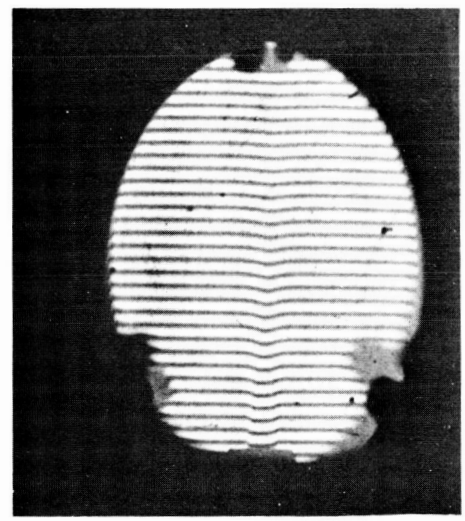

4(b)

FIG. 4 INTERFEROMETER PHOTOGRAPHS OF FLOW FROM A CONVERGENT NOZZLE AT SONIC MACH NUMBER.

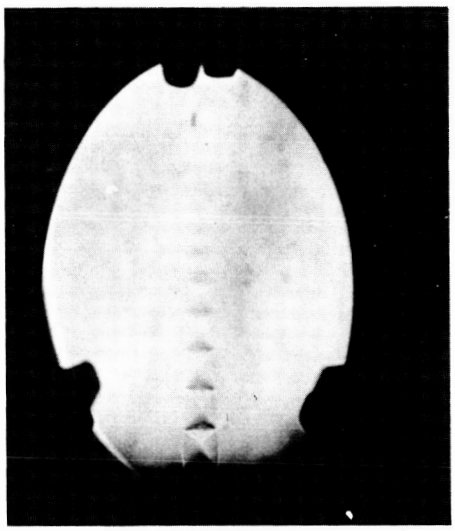

5(a) HORIZONTAL KNIFE EDGE

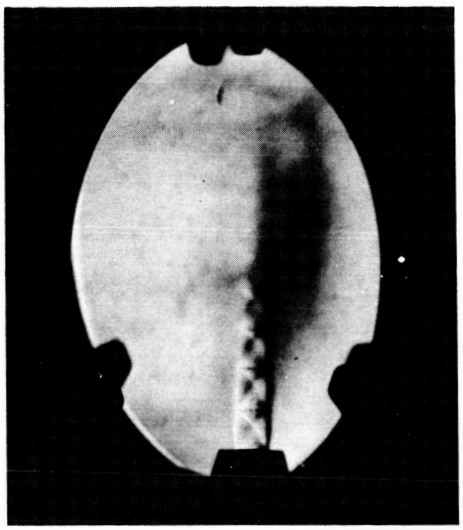

5(b) VERTICAL KNIFE EDGE

FIG. 5 SCHLIEREN PHOTOGRAPHS OF FLOW FROM A CONVERGENT NOZZLE AT MACH NUMBER 1.4

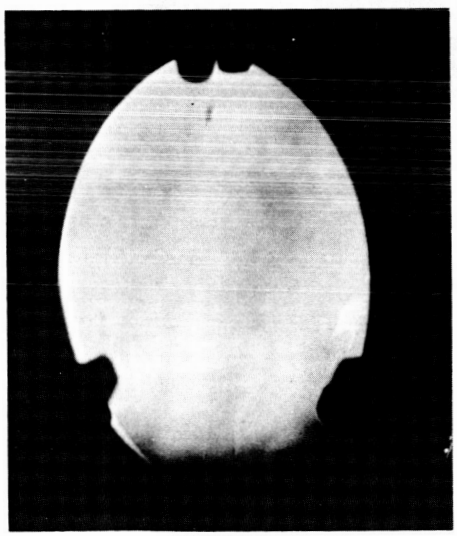

6(a) HORIZONTAL KNIFE EDGE

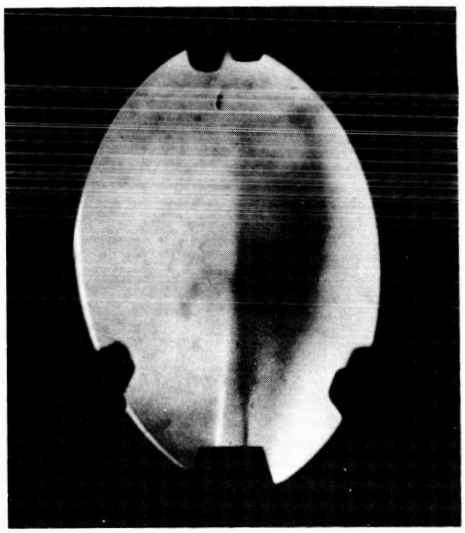

6(b) VERTICAL KNIFE EDGE

FIG. 6 SCHLIEREN PHOTOGRAPHS OF FLOW FROM A CONVERGENT NOZZLE AT SONIC MACH NUMBER.

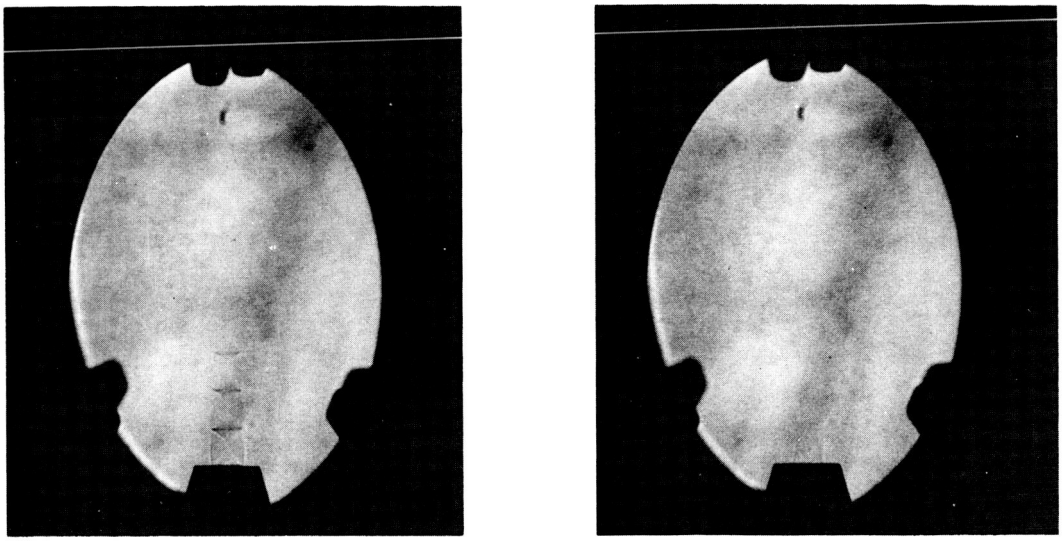

7(a) Mj = 1.4 7(b) Mj = 1.0

FIG. 7 SHADOWGRAPH PHOTOGRAPHS OF FLOW FROM A CONVERGENT NOZZLE AT MACH NUMBERS OF 1.4 AND 1.0

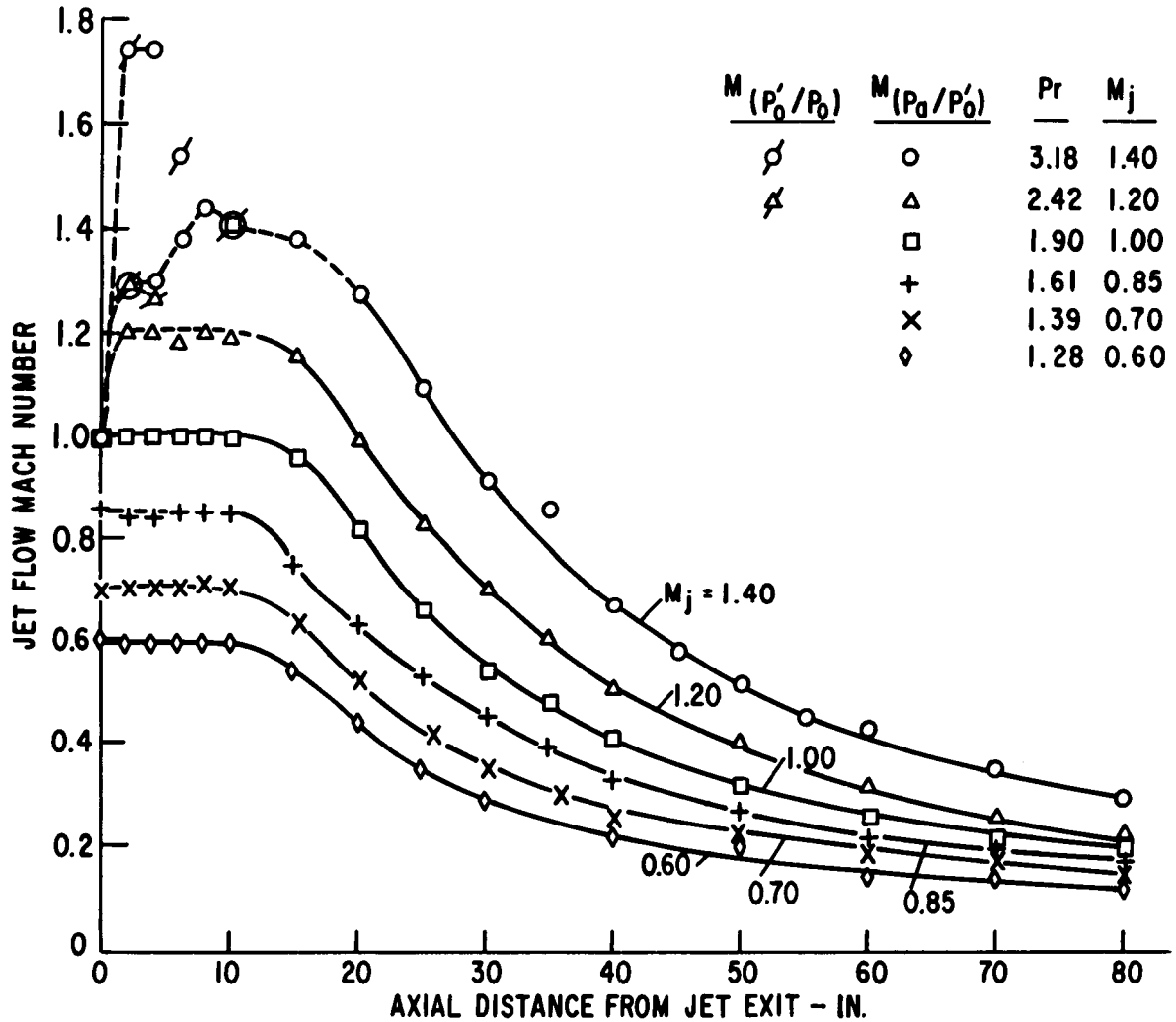

FIG. 8 – VARIATION OF FLOW MACH NUMBER ALONG THE JET AXIS WITH DISTANCE FOR CONVERGENT NOZZLE.

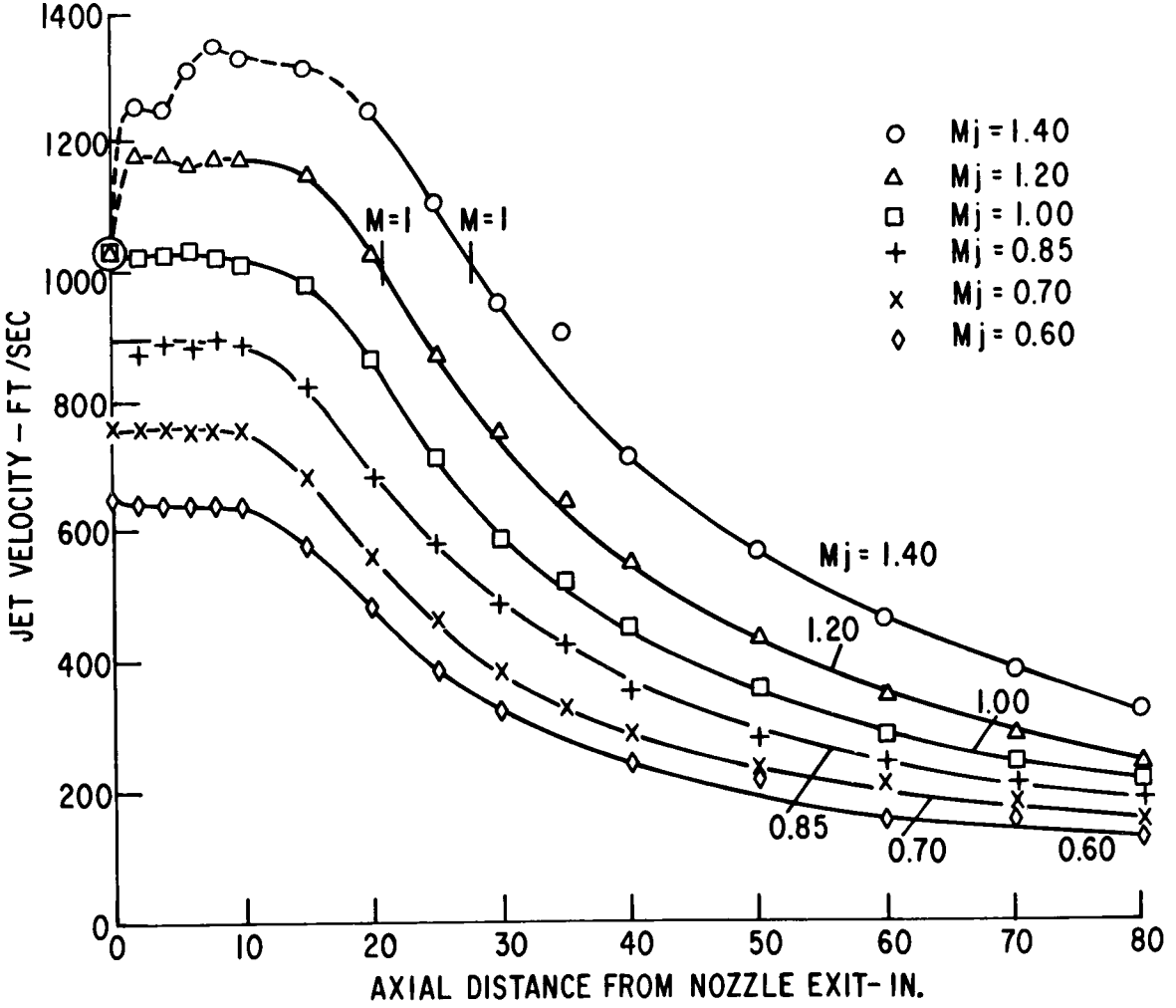

FIG.9-VARIATION OF FLOW VELOCITY ALONG THE JET AXIS WITH DISTANCE FOR CONVERGENT NOZZLE.

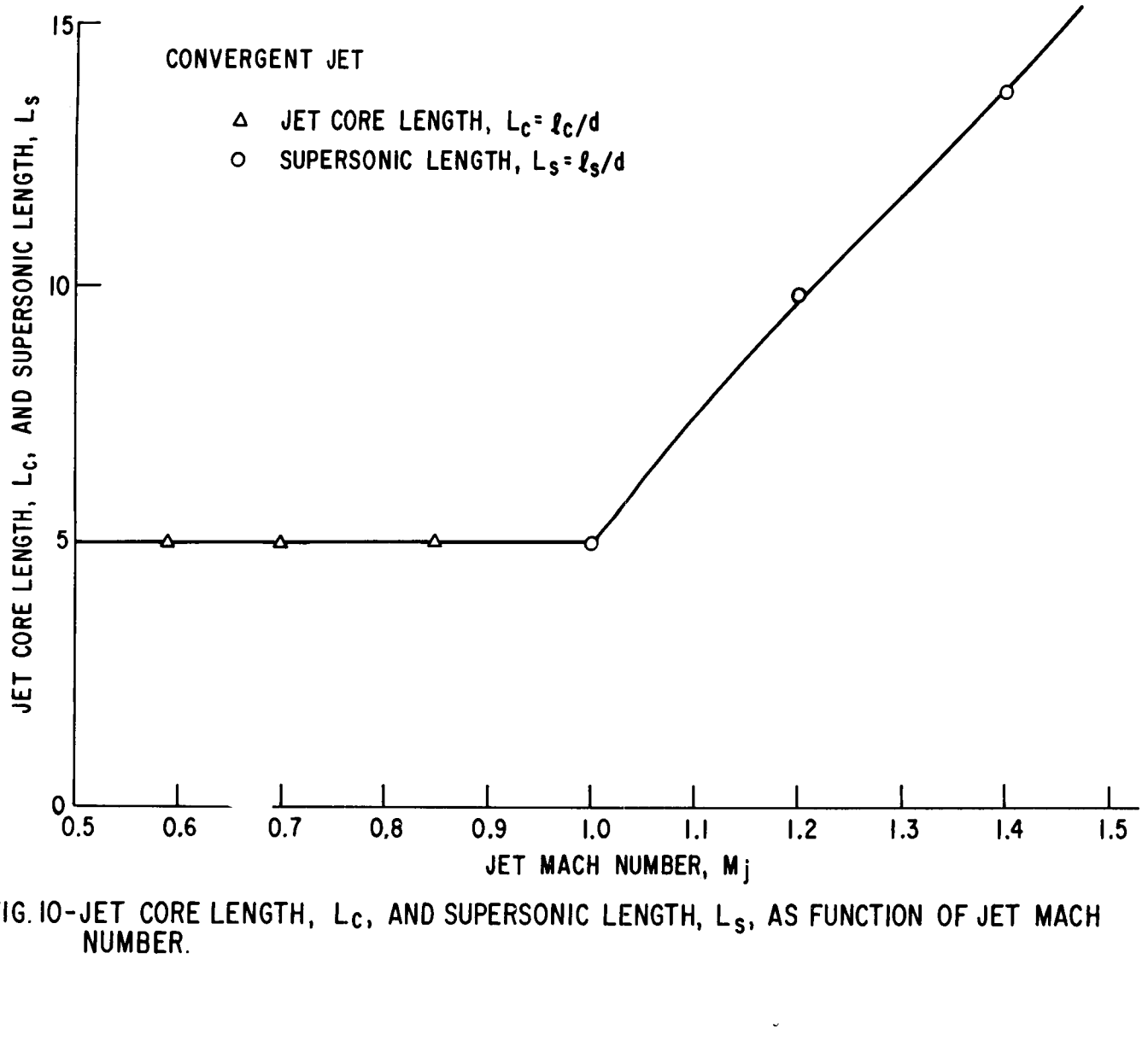

FIG. 10-JET CORE LENGTH, L_c, AND SUPERSONIC LENGTH, L_s, AS FUNCTION OF JET MACH NUMBER.

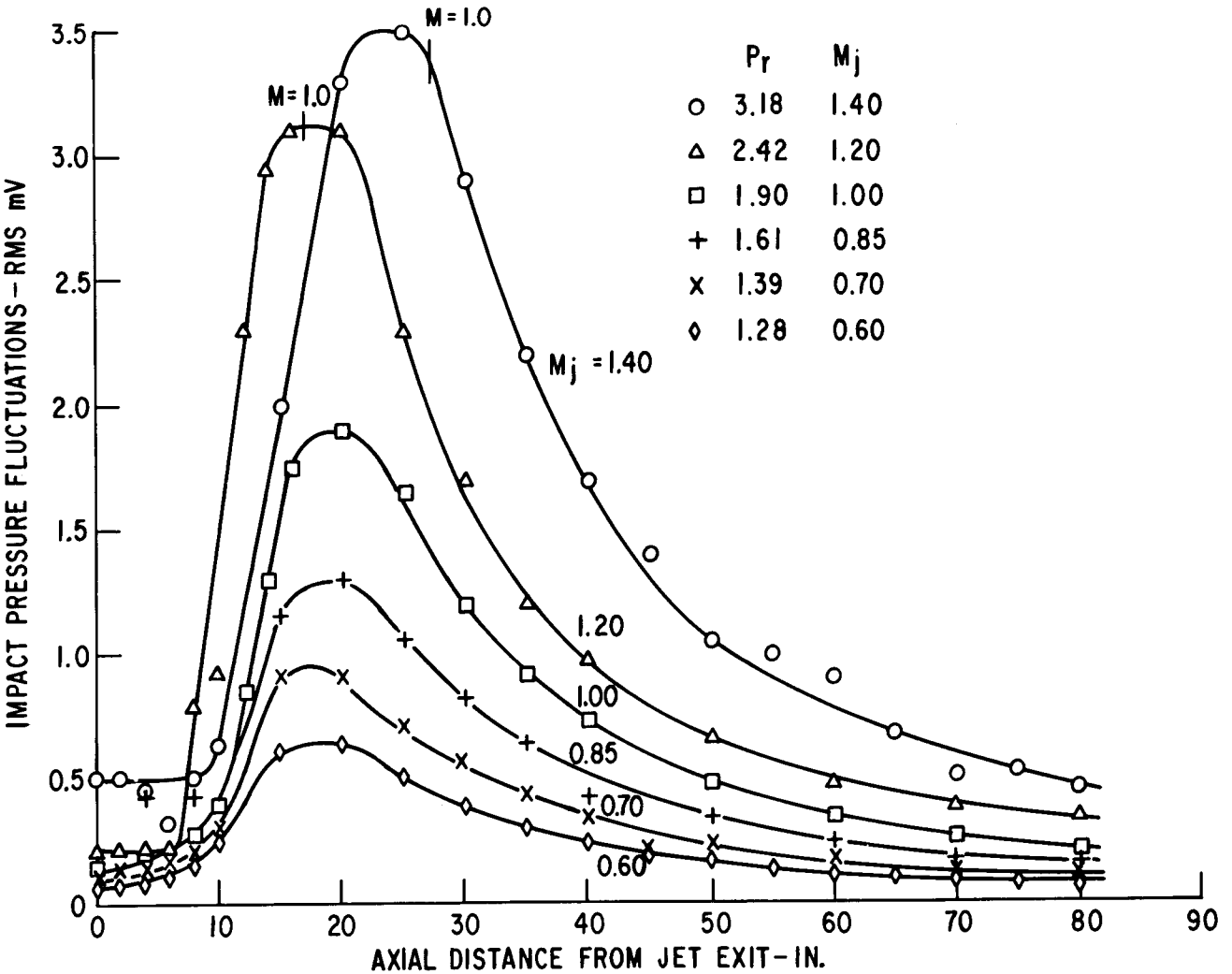

FIG. 11 – IMPACT PRESSURE FLUCTUATIONS ALONG THE JET AXIS FOR CONVERGENT NOZZLE

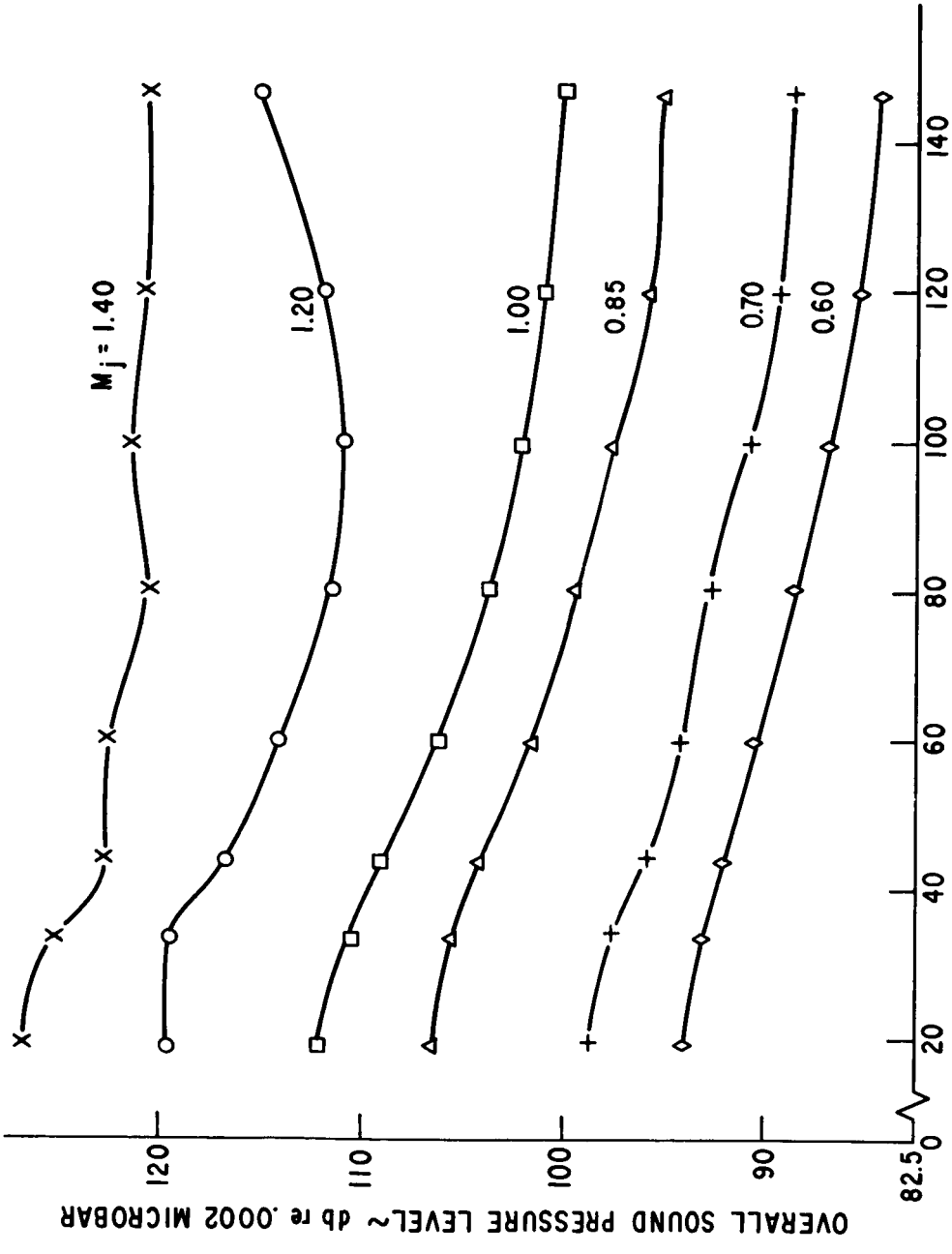

FIG. 12- OVERALL SOUND PRESSURE LEVEL AS A FUNCTION OF ANGULAR POSITION FROM JET AXIS FOR DIFFERENT JET MACH NUMBERS.

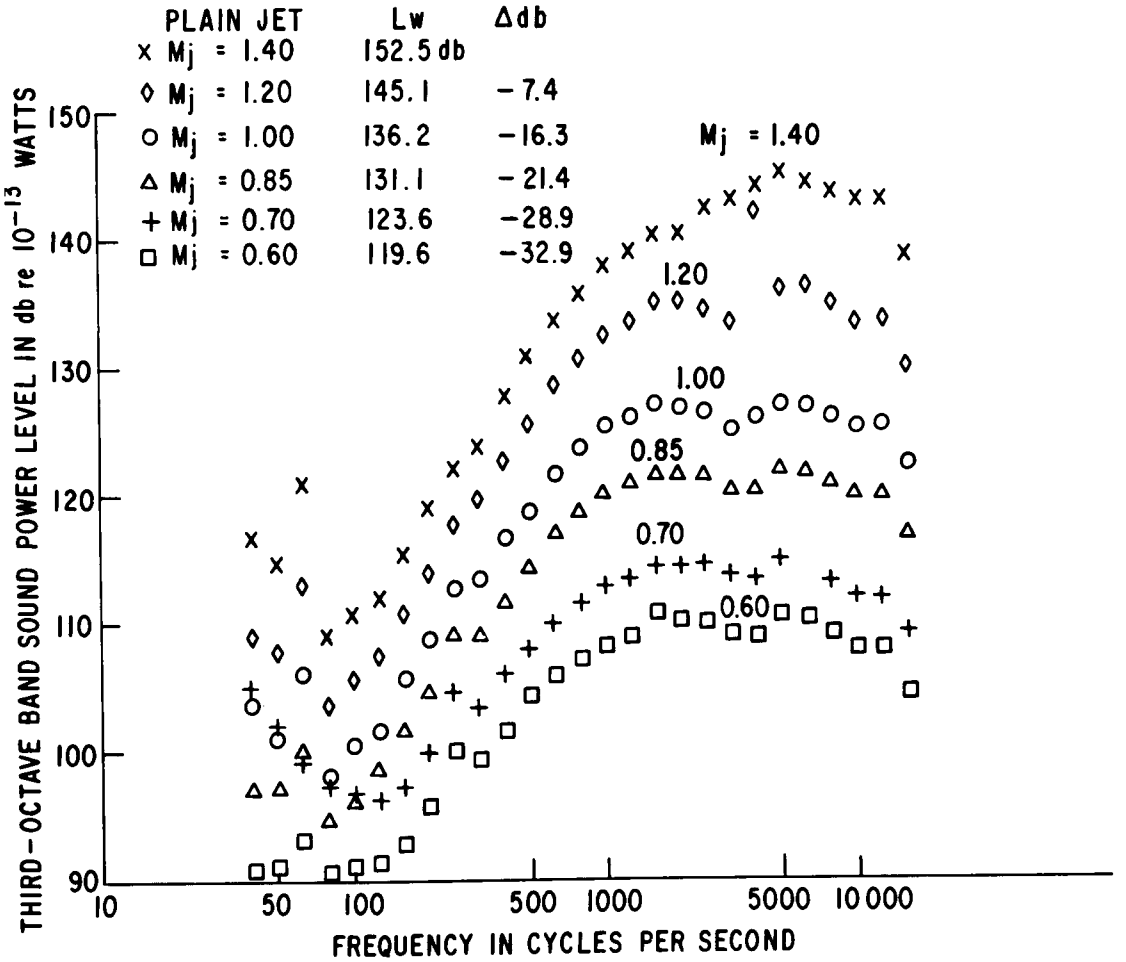

FIG.13-COMPARISON OF SOUND POWER SPECTRA FOR PLAIN CONVERGENT JET AT VARIOUS MACH NUMBERS.

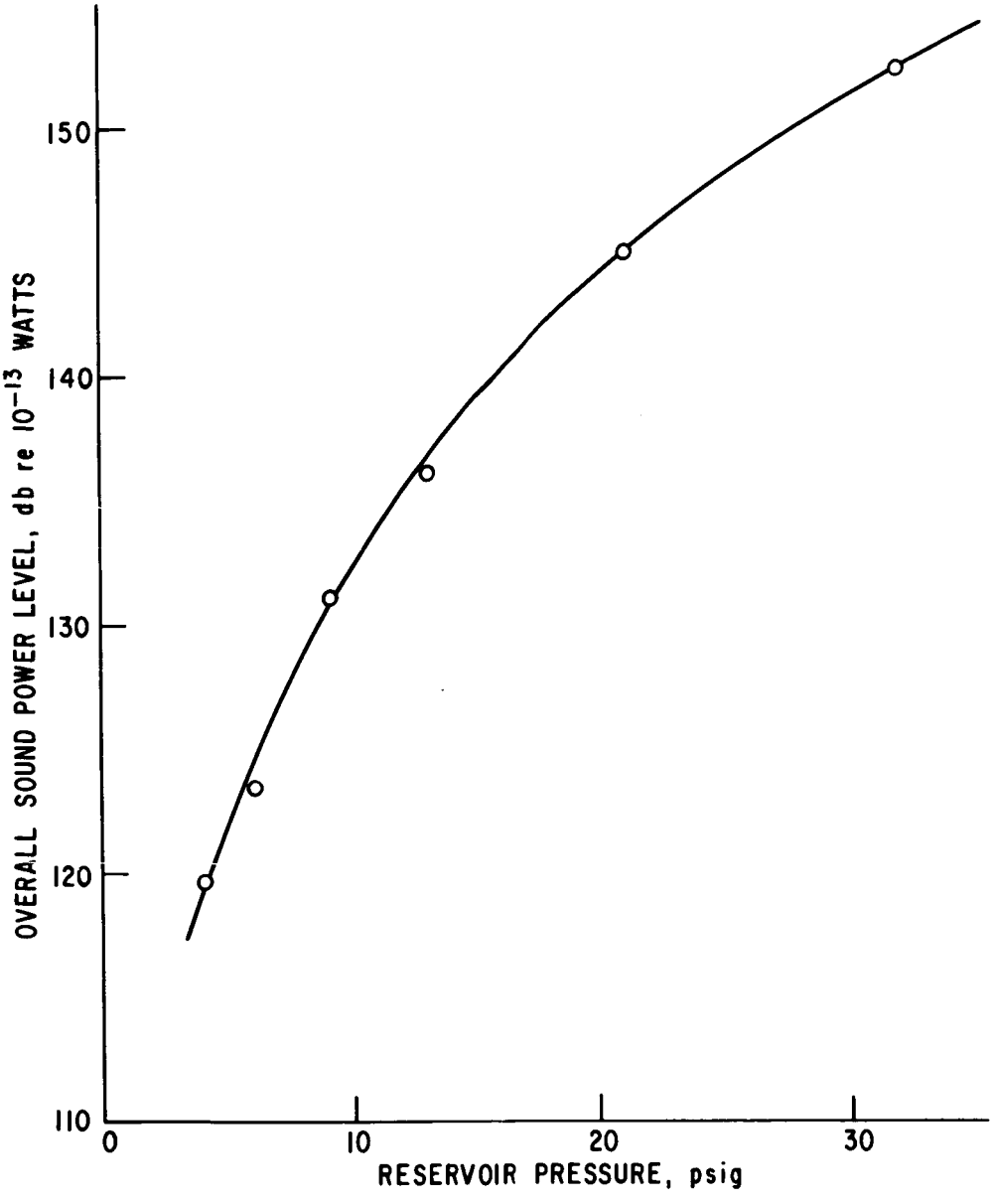

FIG. 14-OVERALL SOUND POWER LEVEL AS FUNCTION OF RESERVOIR PRESSURE FOR CONVERGENT JET.

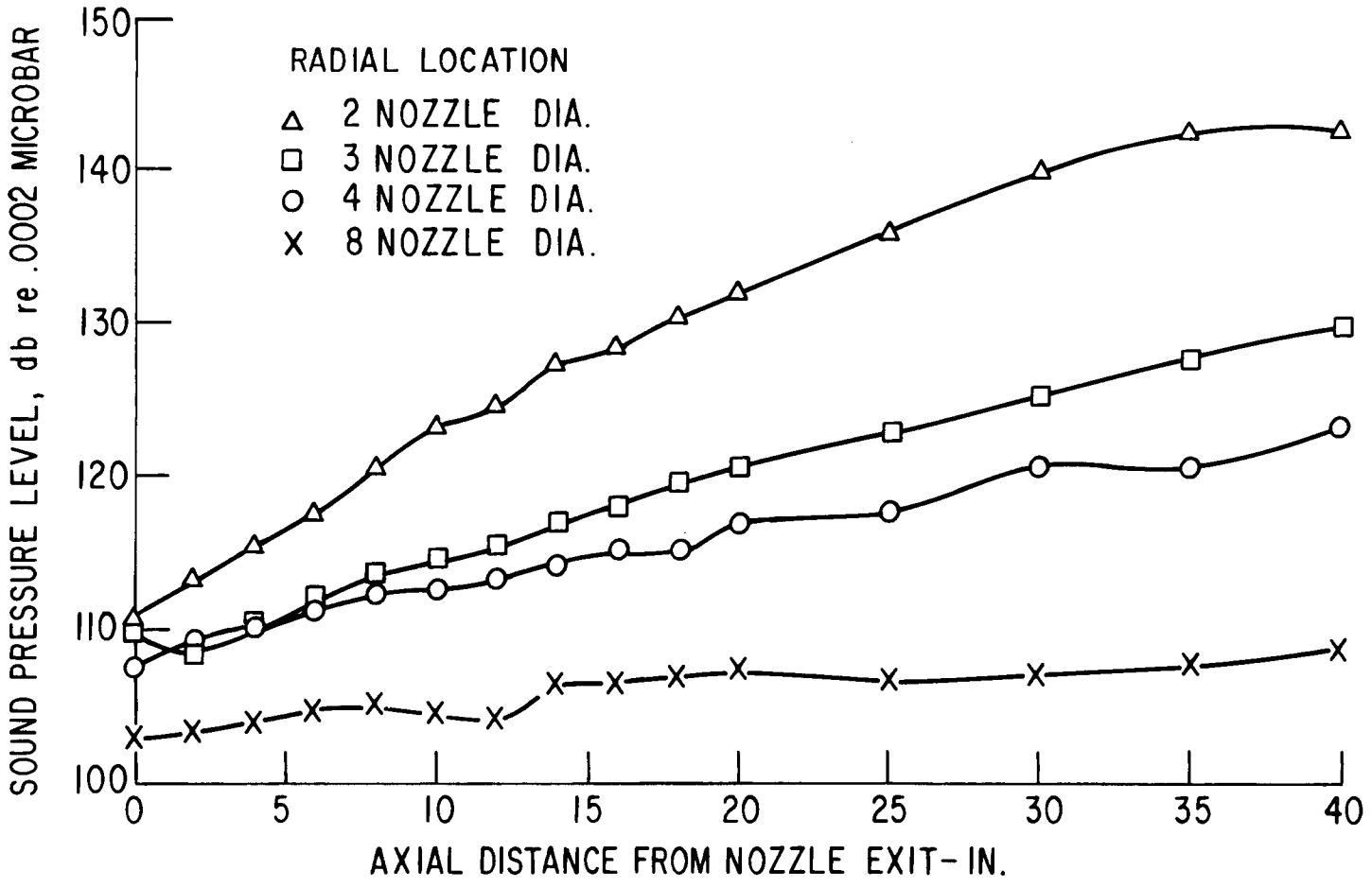

FIG. 15a- NEAR FIELD OVERALL SOUND PRESSURE LEVEL AS A FUNCTION OF RADIAL LOCATION FROM NOZZLE EXIT AND AXIAL DISTANCE FOR JET MACH NUMBER OF 0.60.

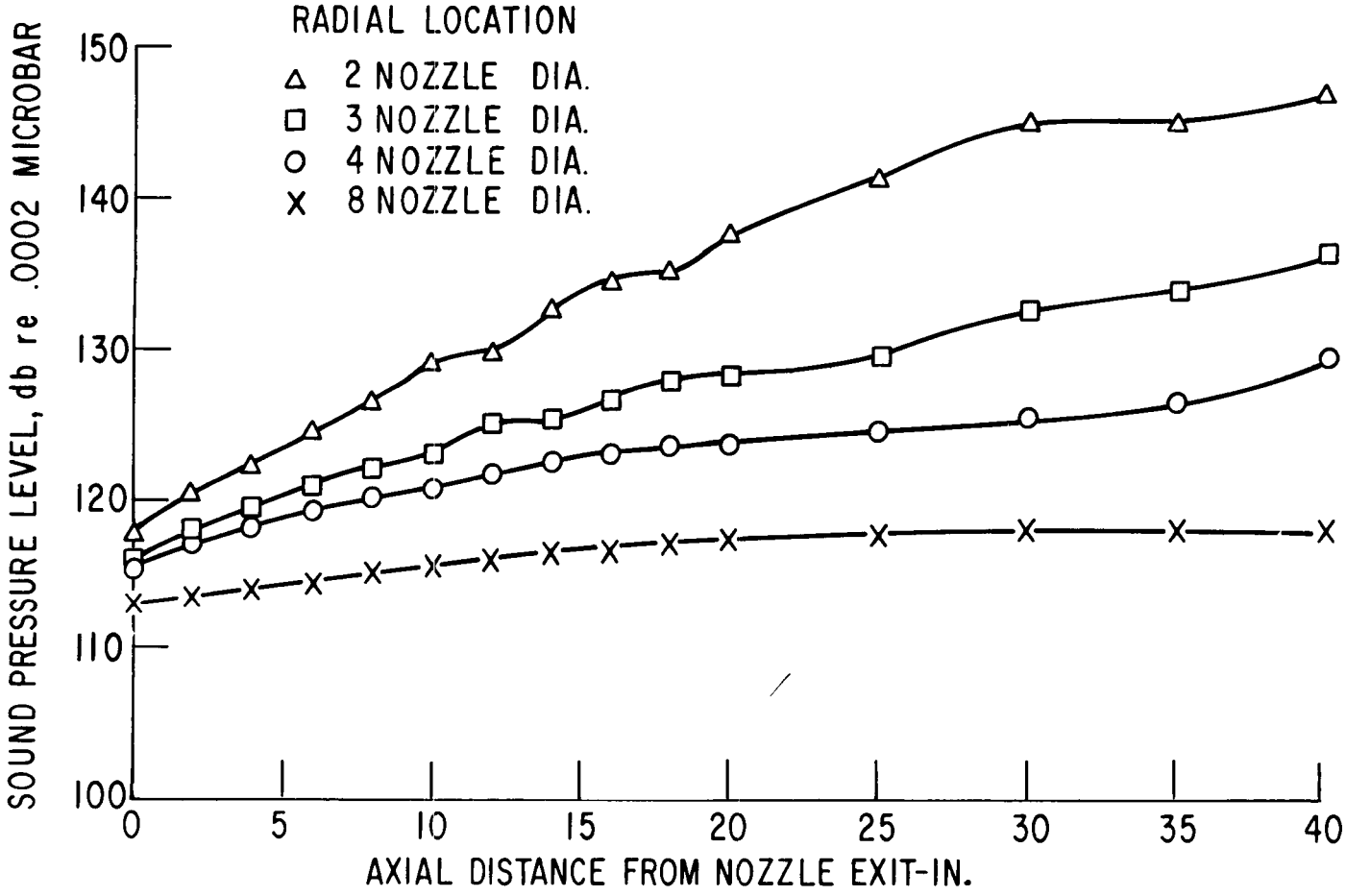

FIG. 15b - NEAR FIELD OVERALL SOUND PRESSURE LEVEL AS A FUNCTION OF RADIAL LOCATION FROM NOZZLE EXIT AND AXIAL DISTANCE FOR JET MACH NUMBER OF 0.85.

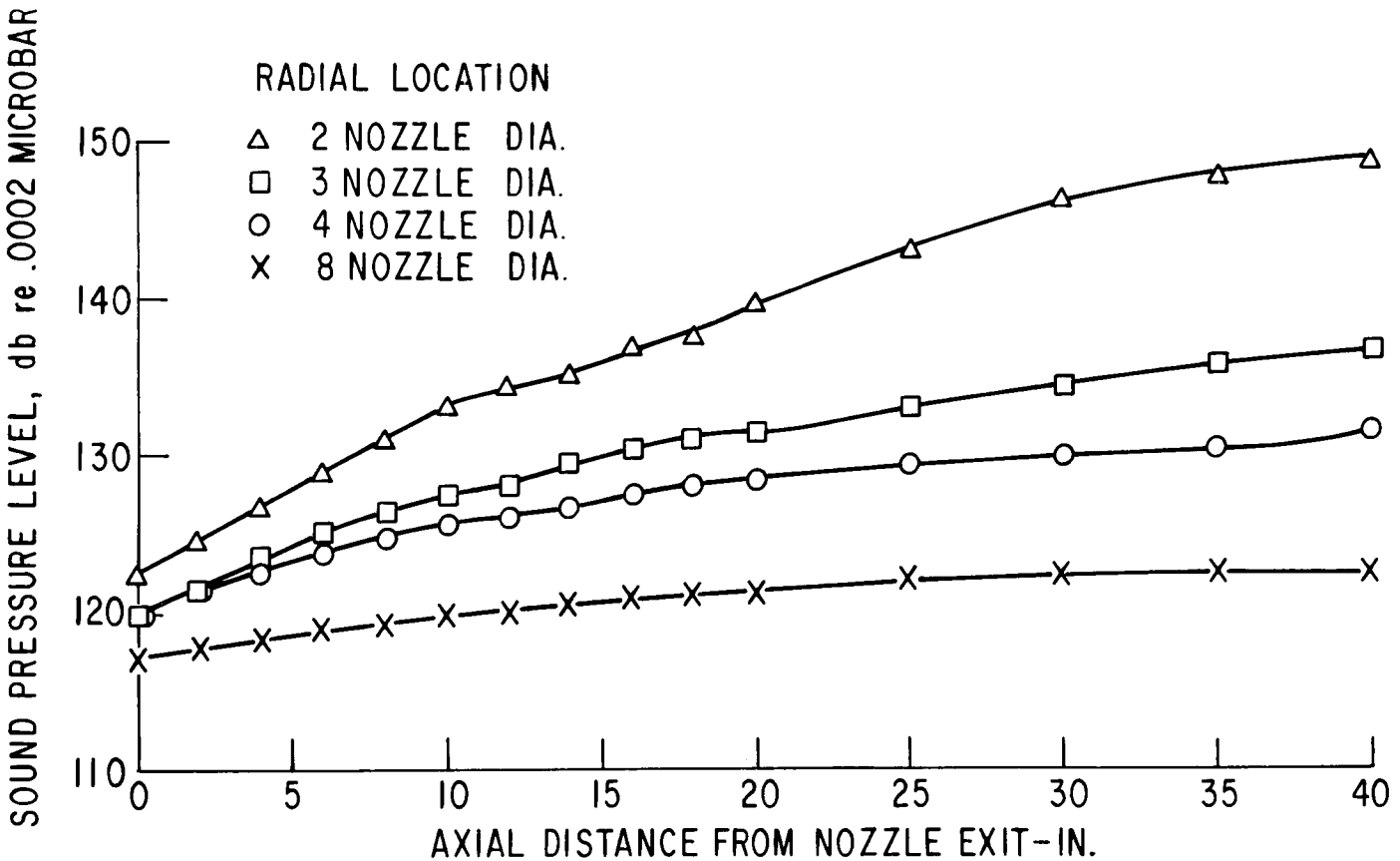

FIG. 15c-NEAR FIELD OVERALL SOUND PRESSURE LEVEL AS A FUNCTION OF RADIAL LOCATION FROM NOZZLE EXIT AND AXIAL DISTANCE FOR JET MACH NUMBER OF 1.00

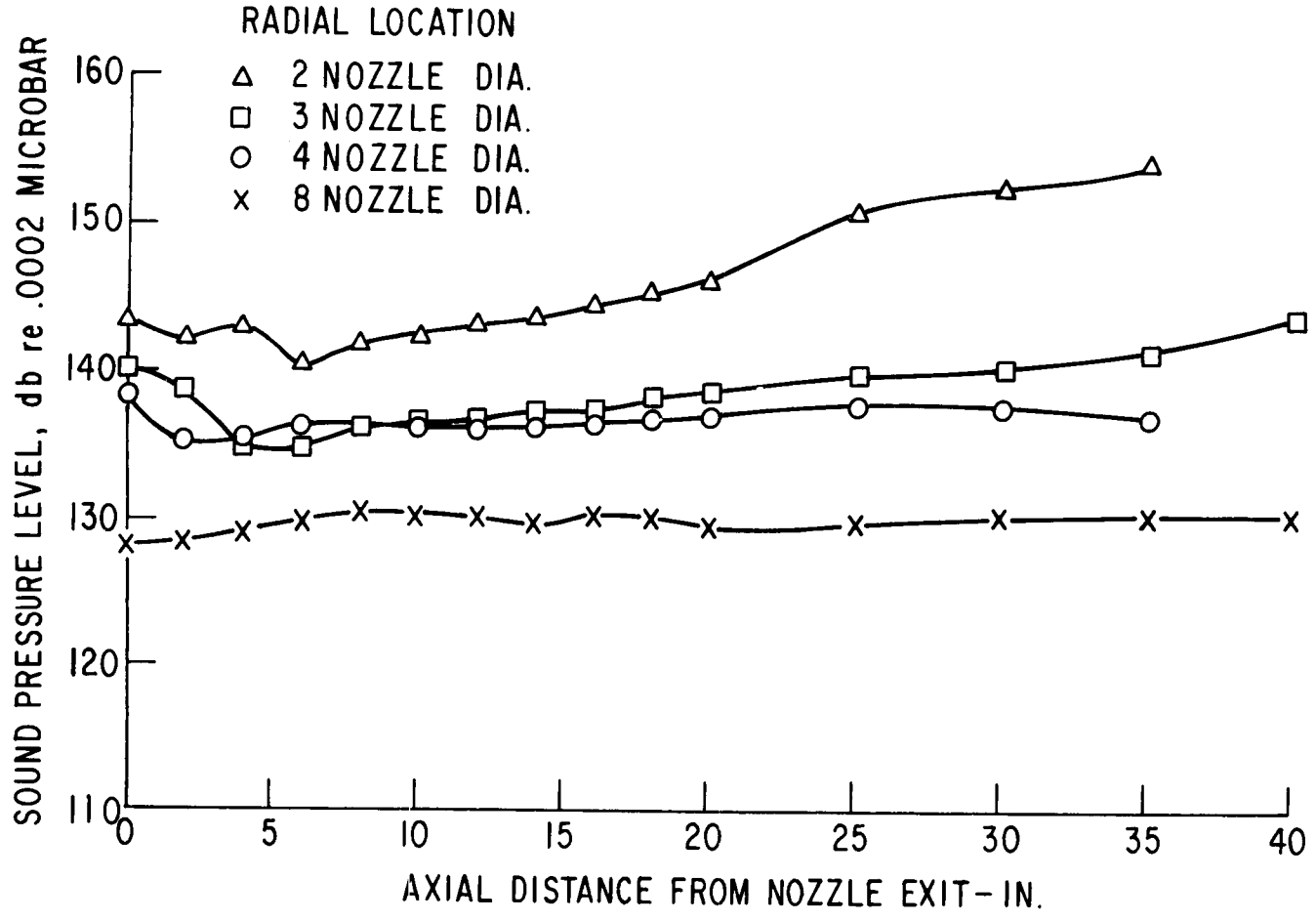

FIG. 15d - NEAR FIELD OVERALL SOUND PRESSURE LEVEL AS A FUNCTION OF RADIAL LOCATION FROM NOZZLE EXIT AND AXIAL DISTANCE FOR JET MACH NUMBER OF 1.20

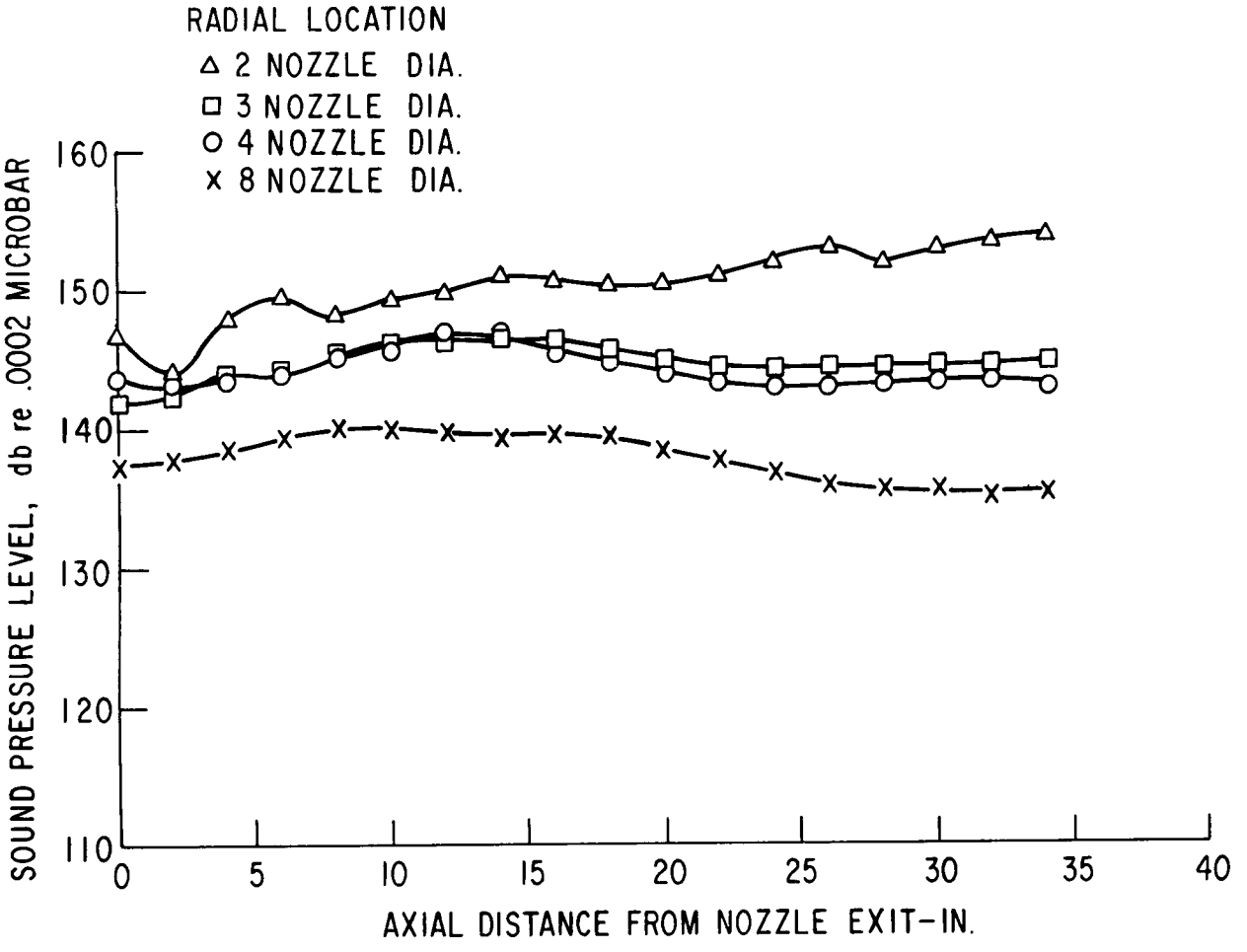

FIG. 15e - NEAR FIELD OVERALL SOUND PRESSURE LEVEL AS A FUNCTION OF RADIAL LOCATION FROM NOZZLE EXIT AND AXIAL DISTANCE FOR JET MACH NUMBER OF 1.40

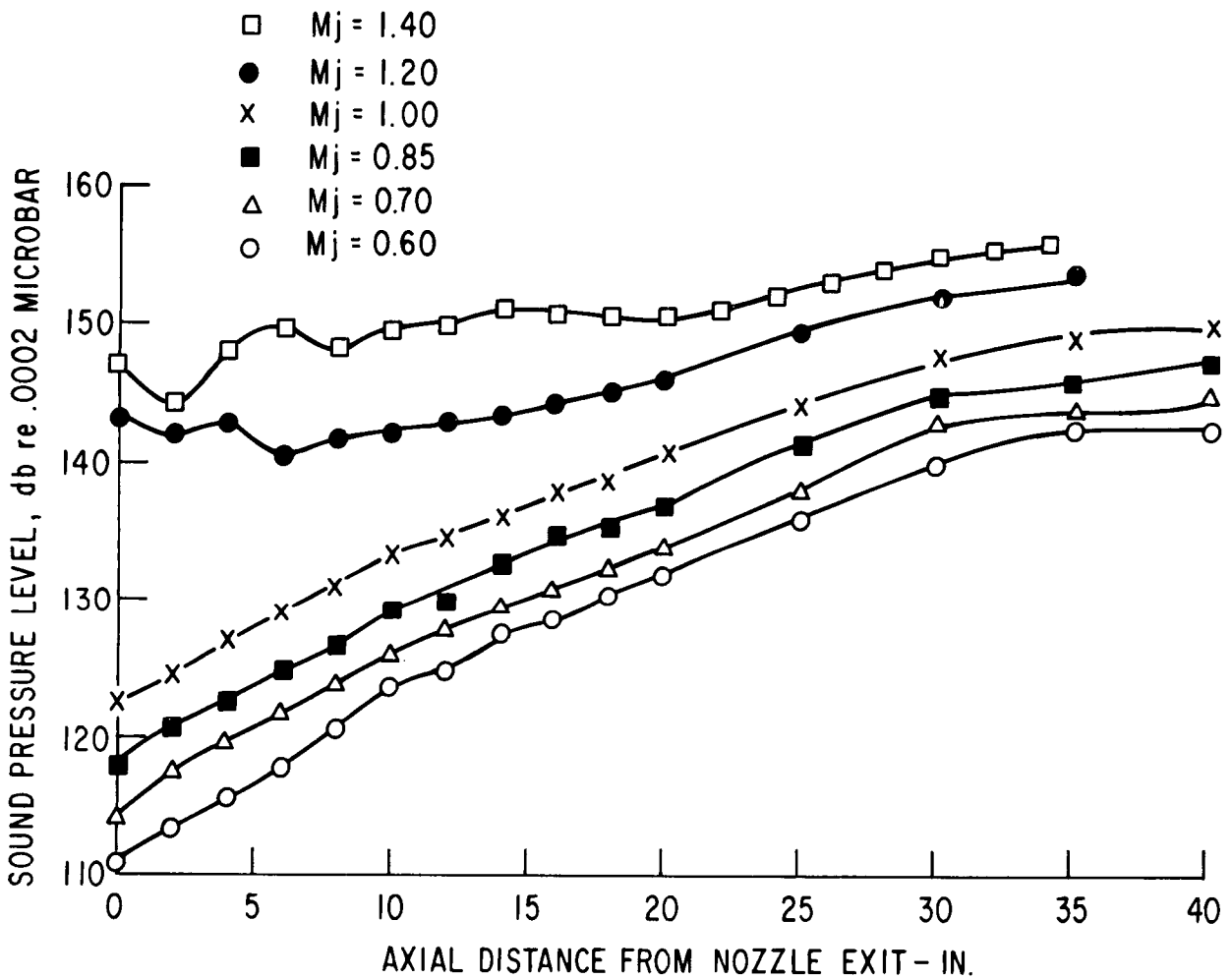

FIG. 16a - NEAR FIELD OVERALL SOUND PRESSURE LEVEL AS A FUNCTION OF JET MACH NUMBER AND AXIAL DISTANCE AT 2 DIAMETERS FROM NOZZLE EXIT.

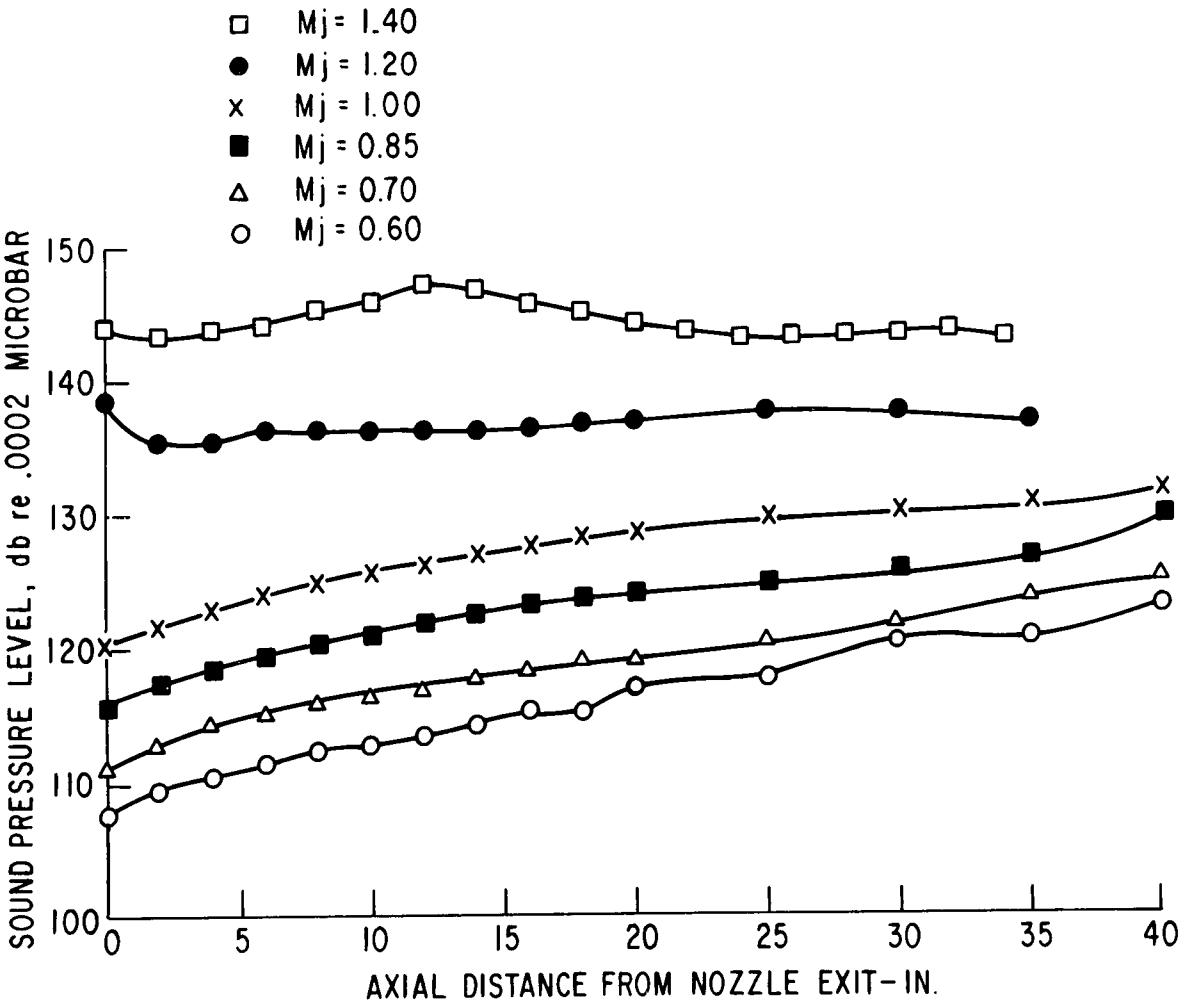

FIG. 16b - NEAR FIELD OVERALL SOUND PRESSURE LEVEL AS A FUNCTION OF JET MACH NUMBER AND AXIAL DISTANCE AT 4 DIAMETERS FROM NOZZLE EXIT.

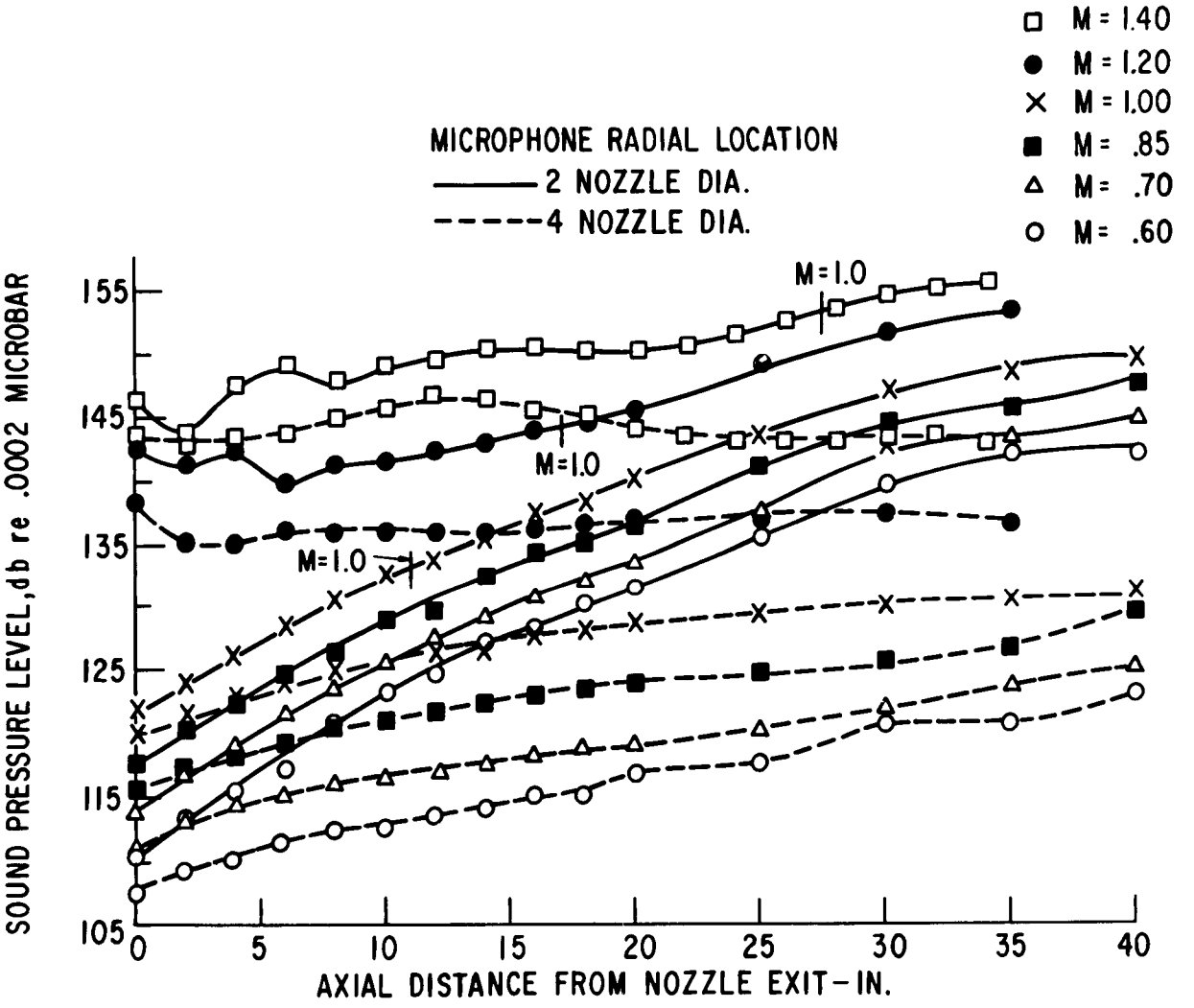

FIG. 16c - SOUND PRESSURE LEVEL VARIATION PARALLEL TO JET AXIS AT 2 AND 4 DIAMETERS FROM NOZZLE EXIT.

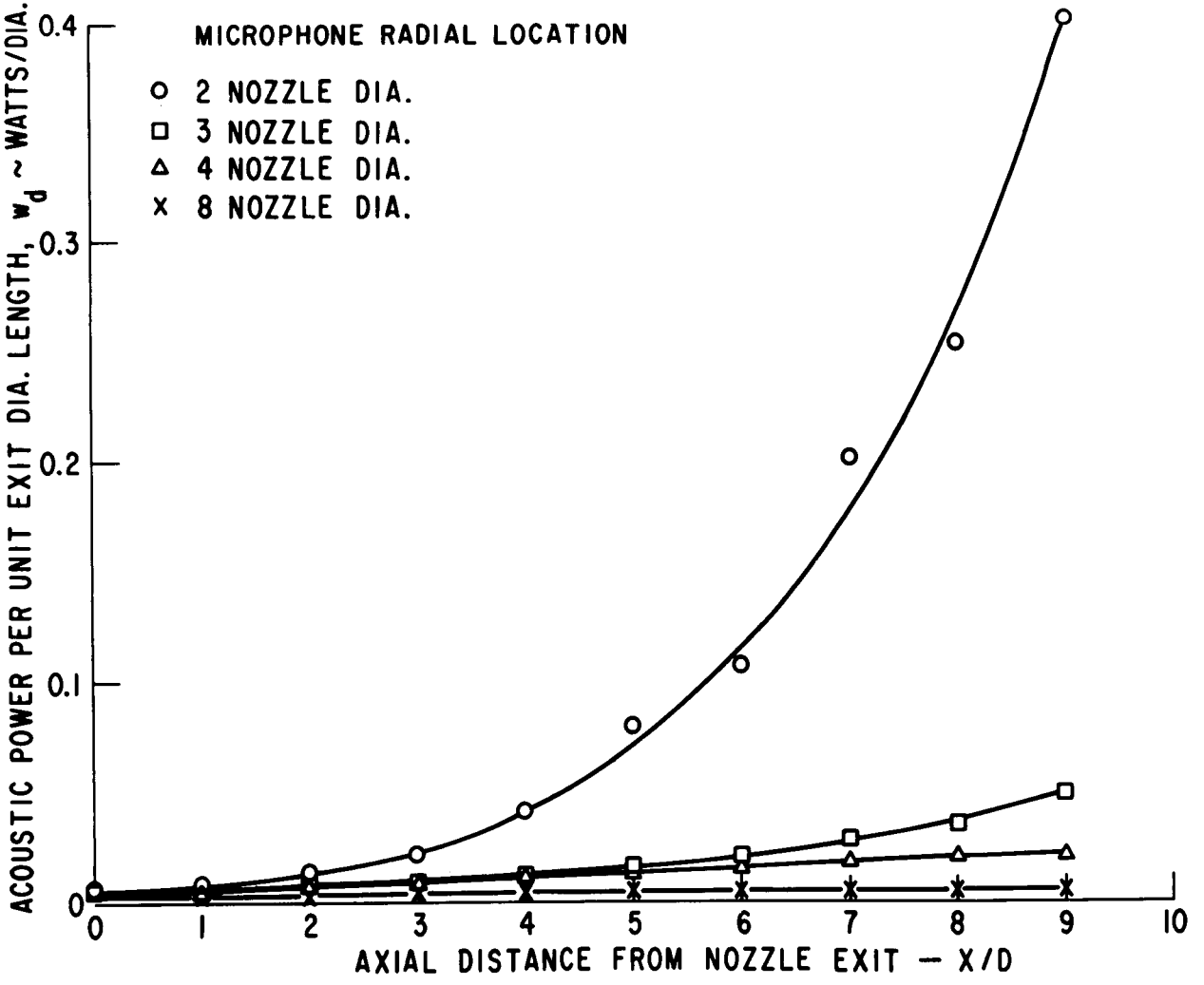

FIG.17a- ACOUSTIC POWER PER UNIT LENGTH OF JET OBTAINED WITH MICROPHONE TRAVERSE PARALLEL TO JET AXIS AND FLOW MACH NUMBER OF 0.60

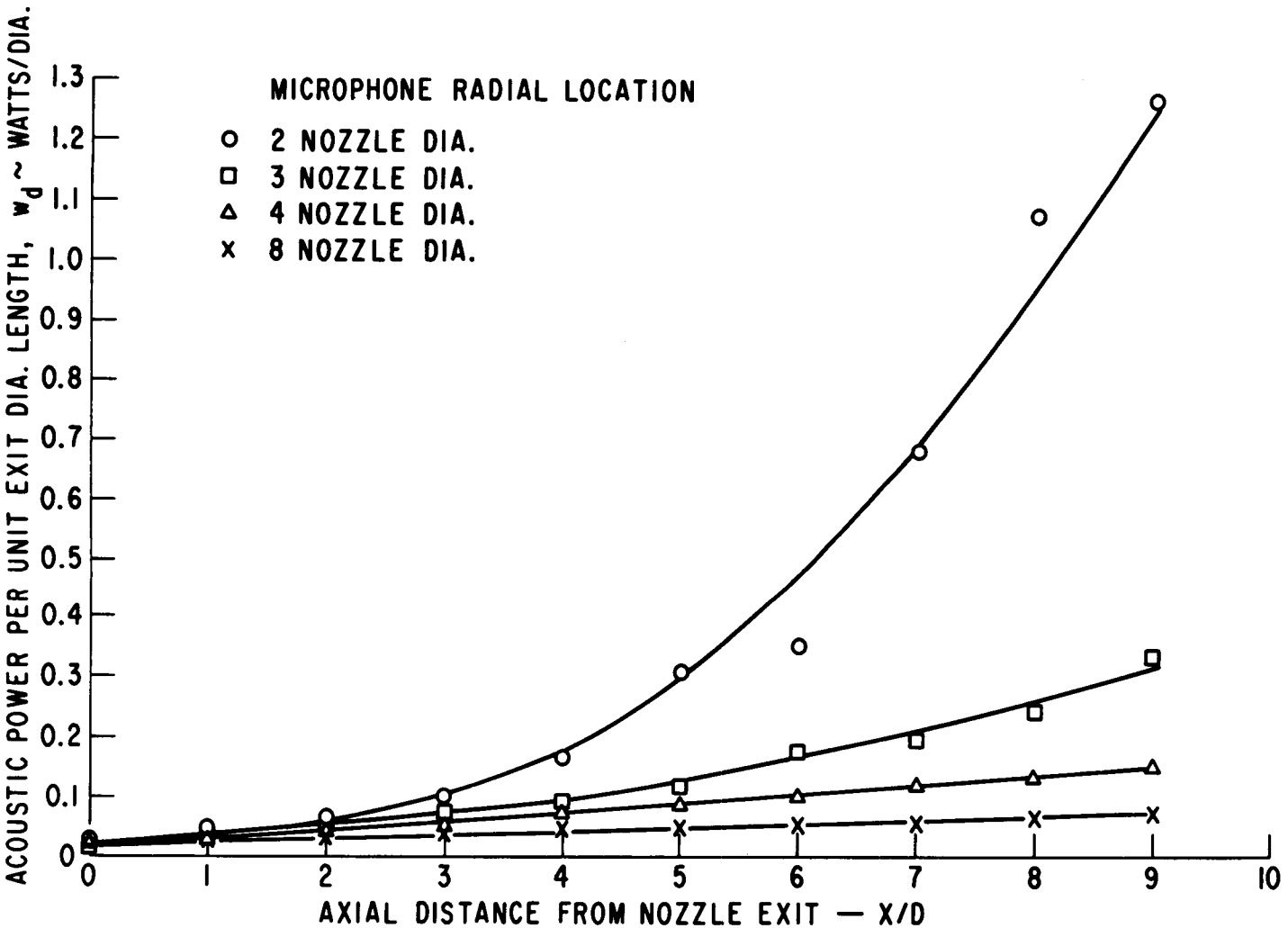

FIG.17b-ACOUSTIC POWER PER UNIT LENGTH OF JET OBTAINED WITH MICROPHONE TRAVERSE PARALLEL TO JET AXIS AND FLOW MACH NUMBER OF 0.85

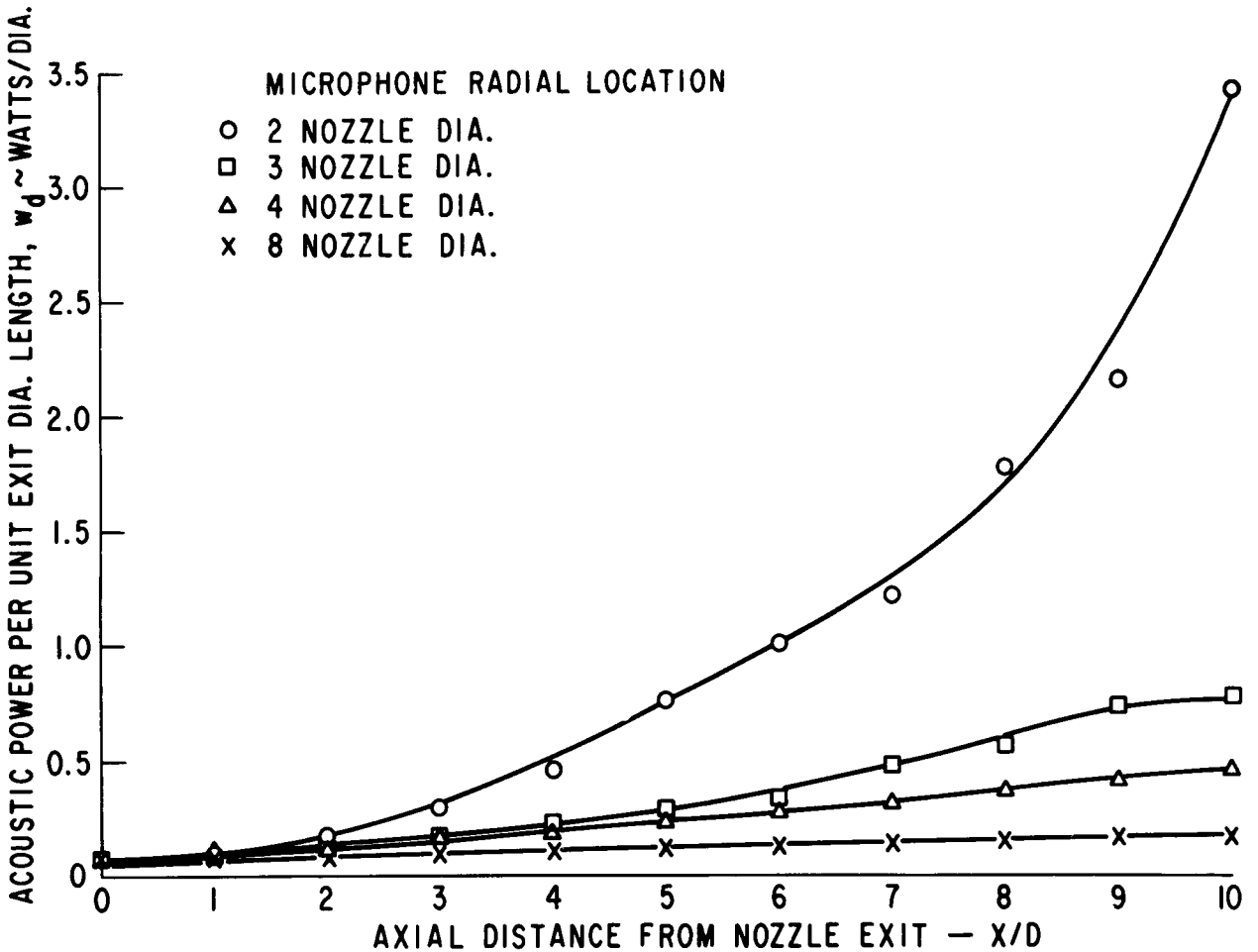

FIG. 17c - ACOUSTIC POWER PER UNIT LENGTH OF JET OBTAINED WITH MICROPHONE TRAVERSE PARALLEL TO JET AXIS AND FLOW MACH NUMBER OF 1.00

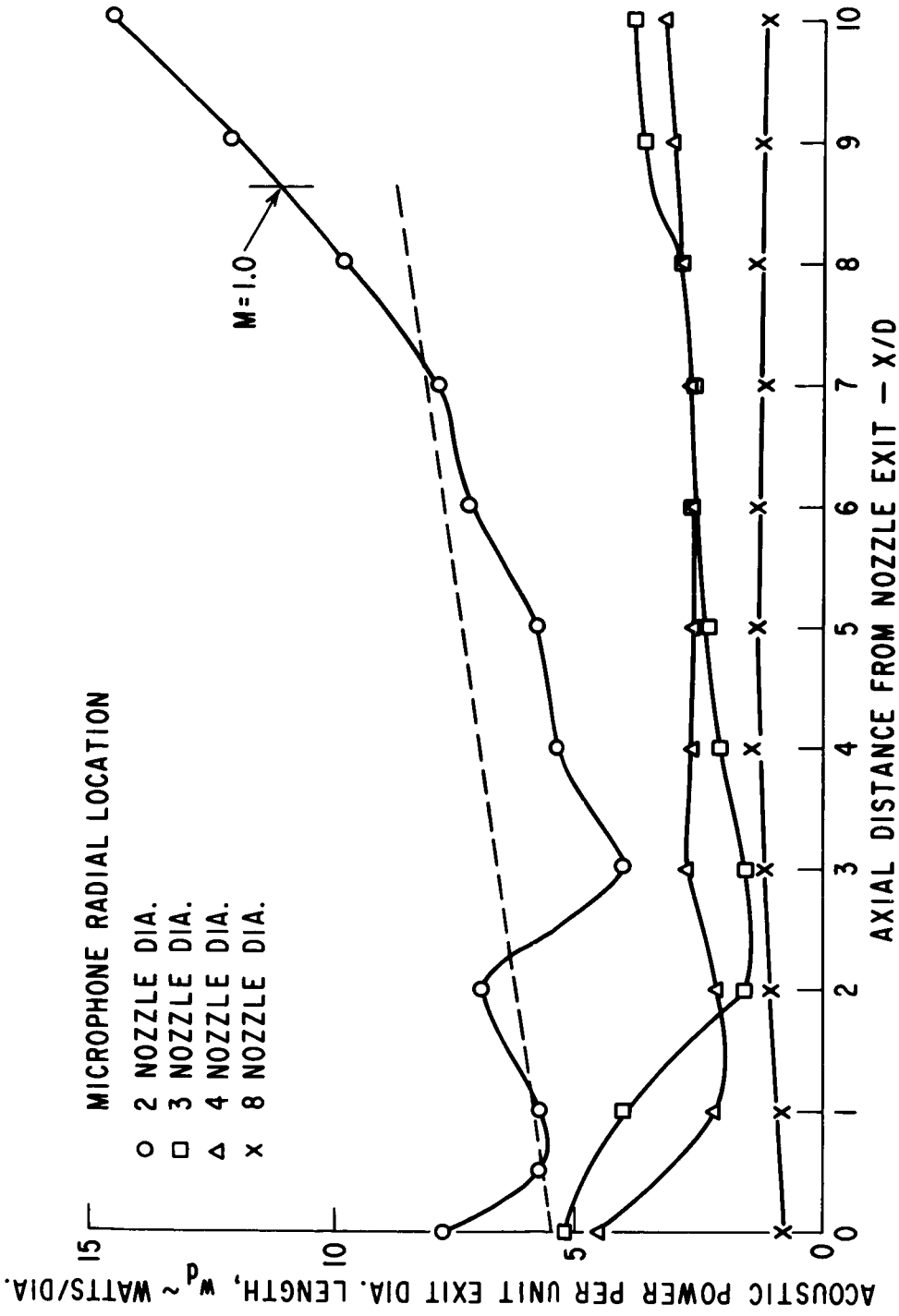

FIG. 17d– ACOUSTIC POWER PER UNIT LENGTH OF JET OBTAINED WITH MICROPHONE TRAVERSE PARALLEL TO JET AXIS AND FLOW MACH NUMBER OF 1.20

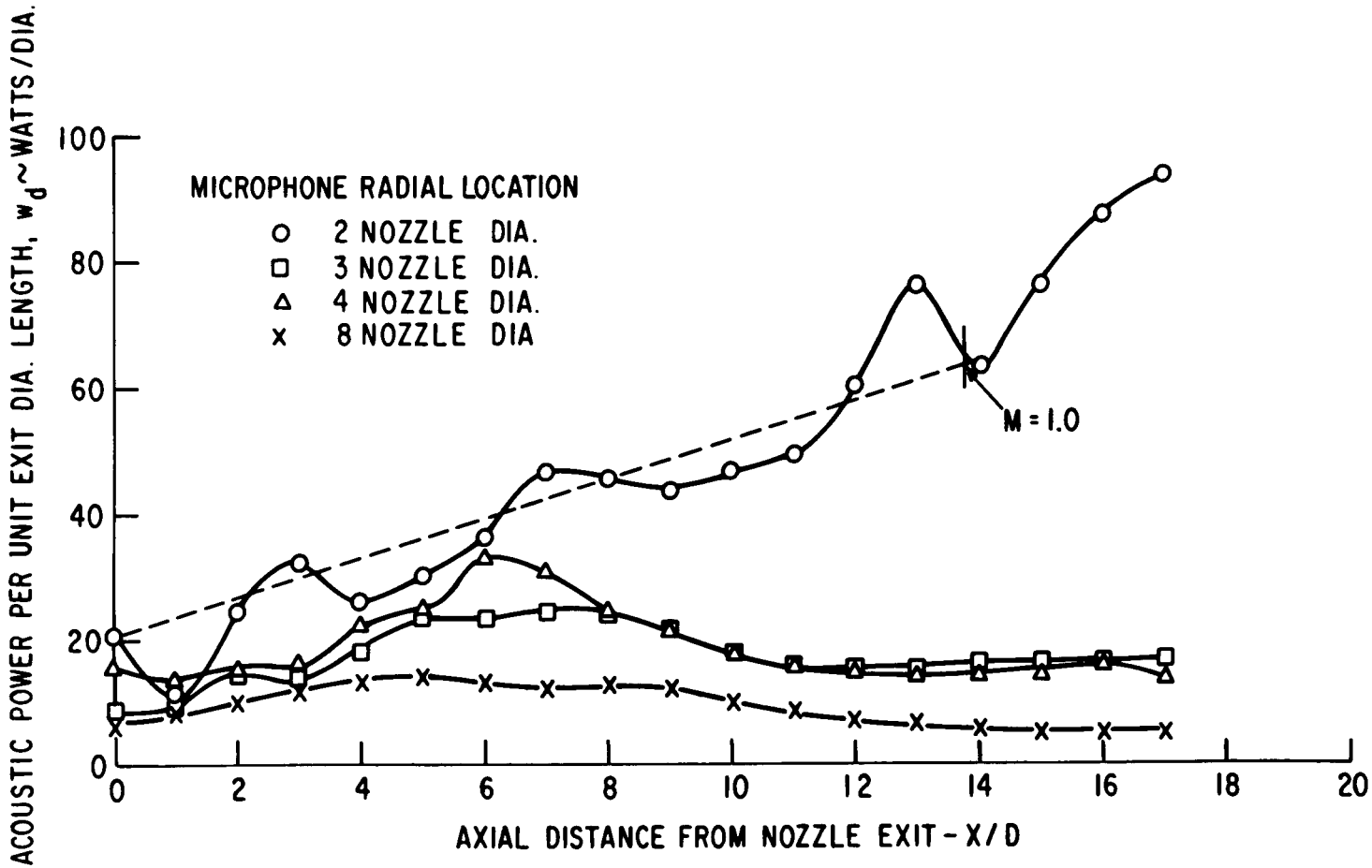

FIG. 17e-ACOUSTIC POWER PER UNIT LENGTH OF JET OBTAINED WITH MICROPHONE TRAVERSE PARALLEL TO JET AXIS AND FLOW MACH NUMBER OF 1.40

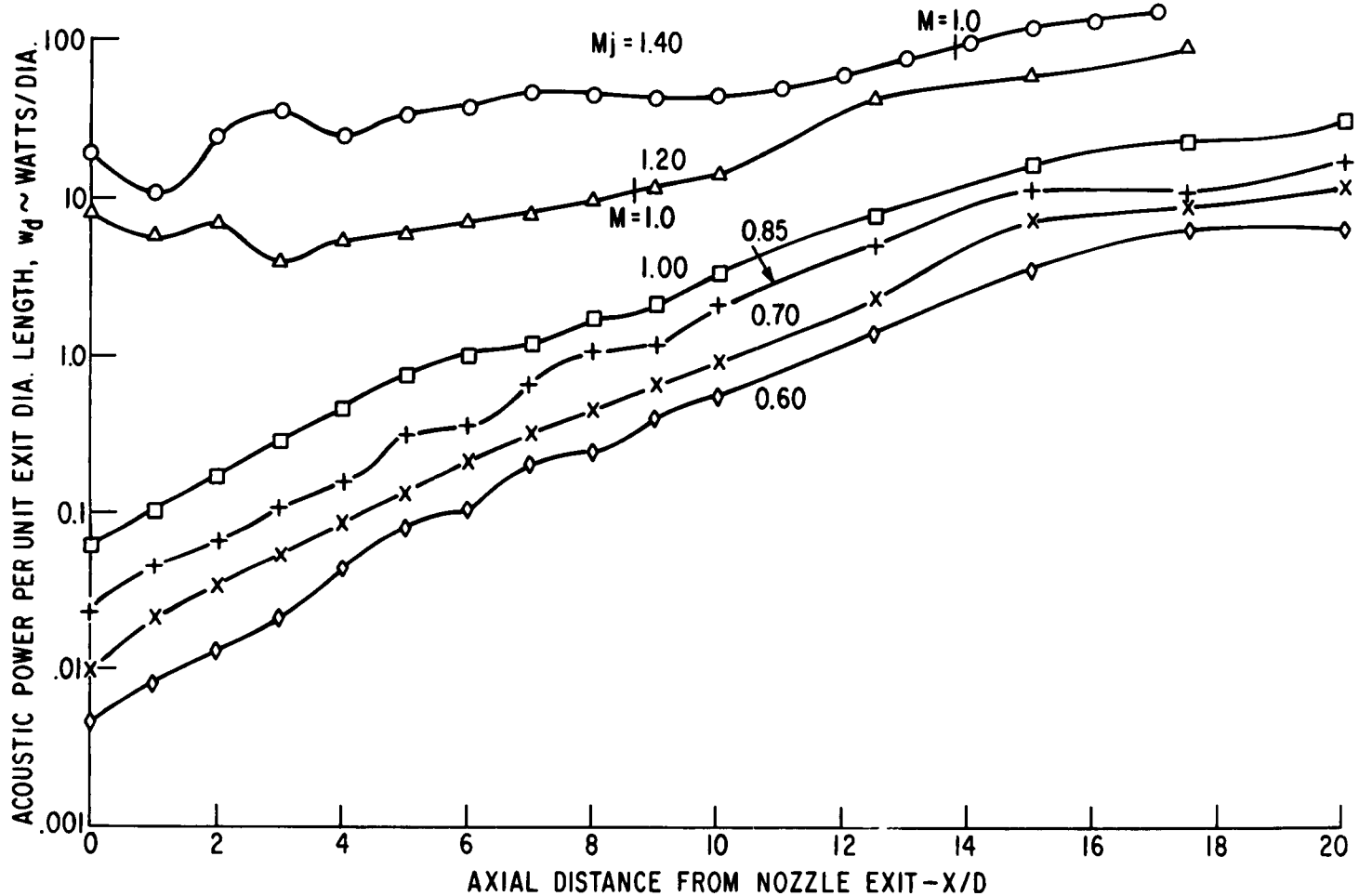

FIG. 18a-ACOUSTIC POWER PER UNIT LENGTH OF JET OBTAINED WITH MICROPHONE TRAVERSE PARALLEL TO JET AXIS TWO NOZZLE DIAMETERS FROM NOZZLE PERIPHERY.

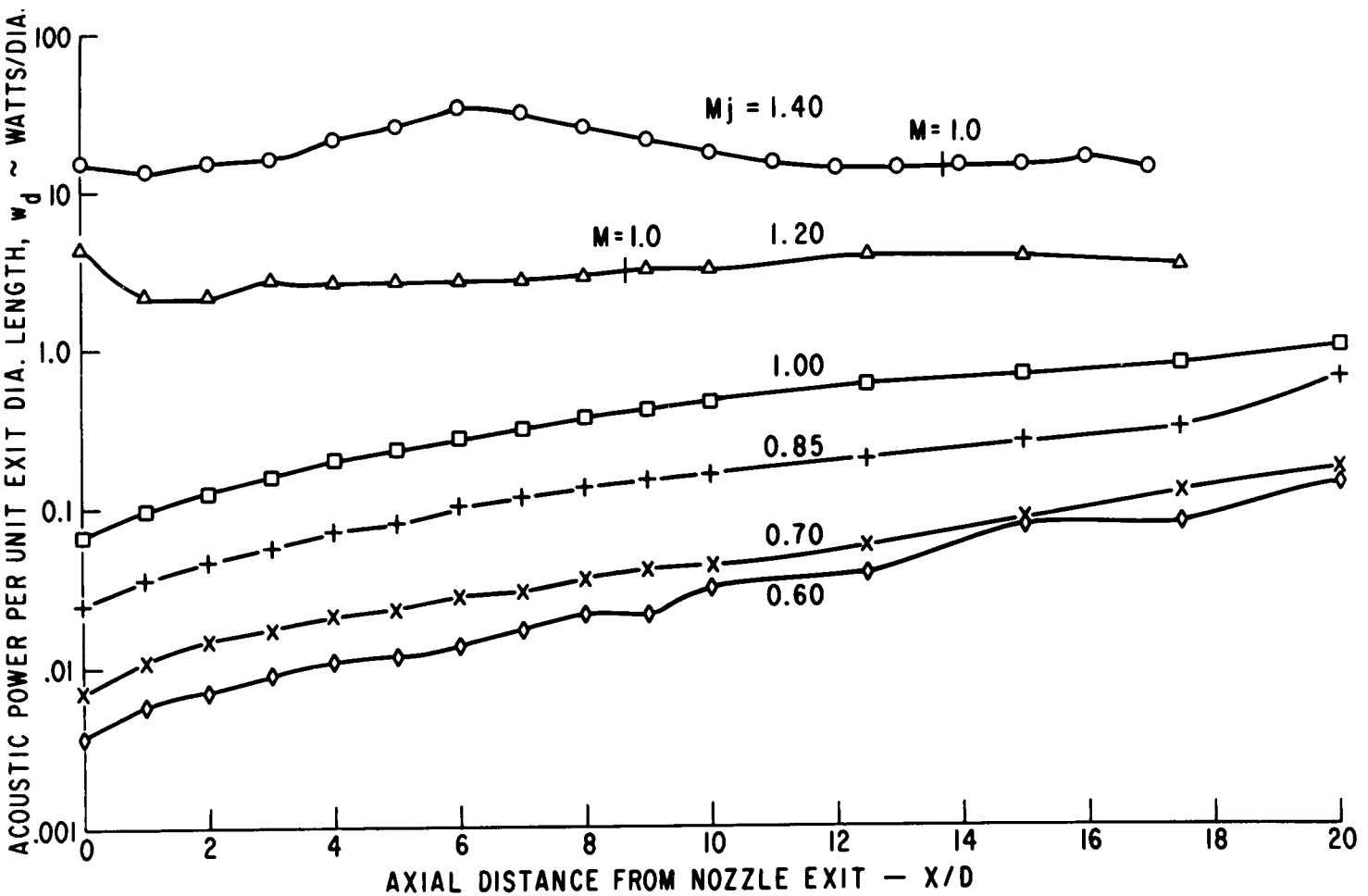

FIG. 18b - ACOUSTIC POWER PER UNIT LENGTH OF JET OBTAINED WITH MICROPHONE TRAVERSE PARALLEL TO JET AXIS FOUR NOZZLE DIAMETERS FROM NOZZLE PERIPHERY.

OVERALL ACOUSTIC POWER LEVEL	Mj = 1.00	Mj = 0.85
L_w INTEGRATED OVER 2 NOZZLE DIA. CYLINDER	134	129
L_w INTEGRATED OVER 10 FT. RADIUS SPHERE	140	135

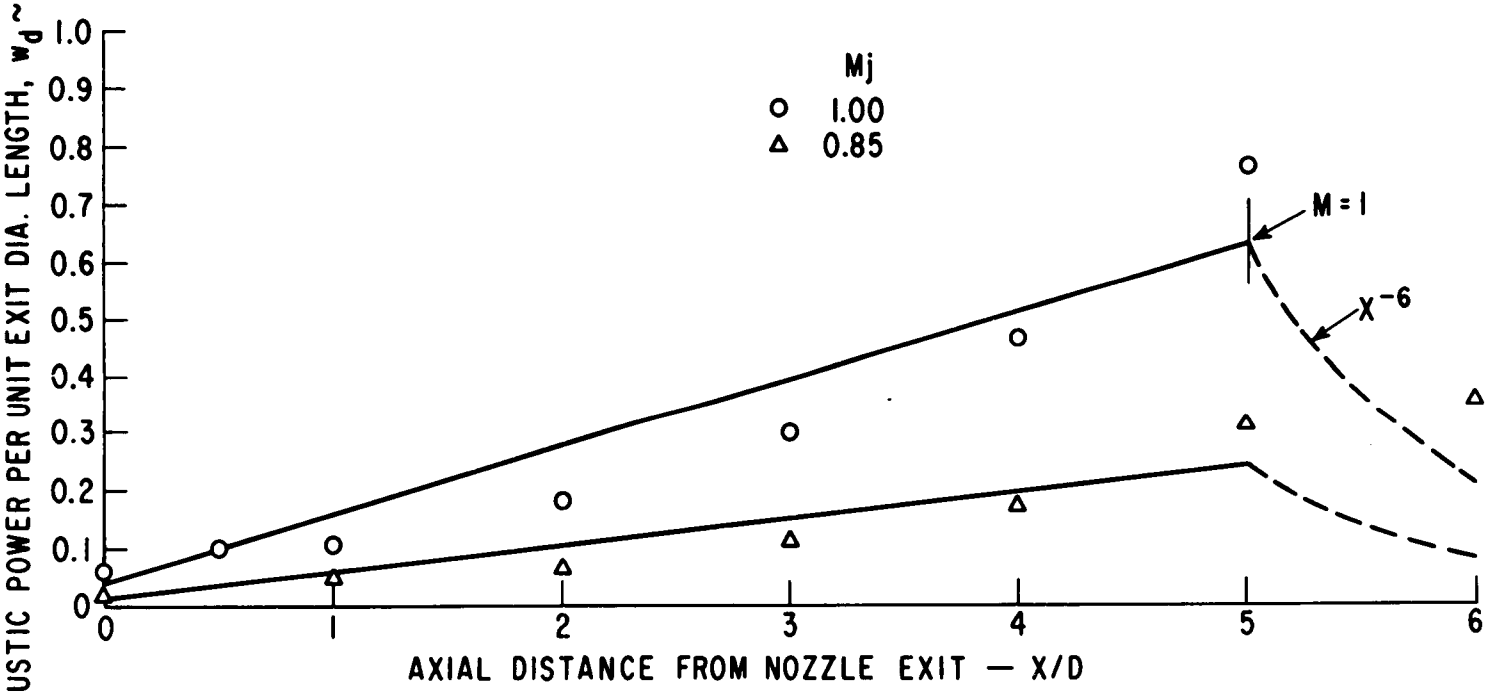

FIG. 19a – ACOUSTIC POWER PER UNIT LENGTH OF JET OBTAINED WITH MICROPHONE TRAVERSE PARALLEL TO JET AXIS AT TWO NOZZLE DIAMETERS FROM NOZZLE PERIPHERY

OVERALL ACOUSTIC POWER LEVEL	Mj=1.4	Mj=1.2
L_w – INTEGRATED OVER 2 NOZZLE DIA. CYLINDER	158 db	149 db
L_w – INTEGRATED OVER 10FT. RADIUS SPHERE	156 db	148 db

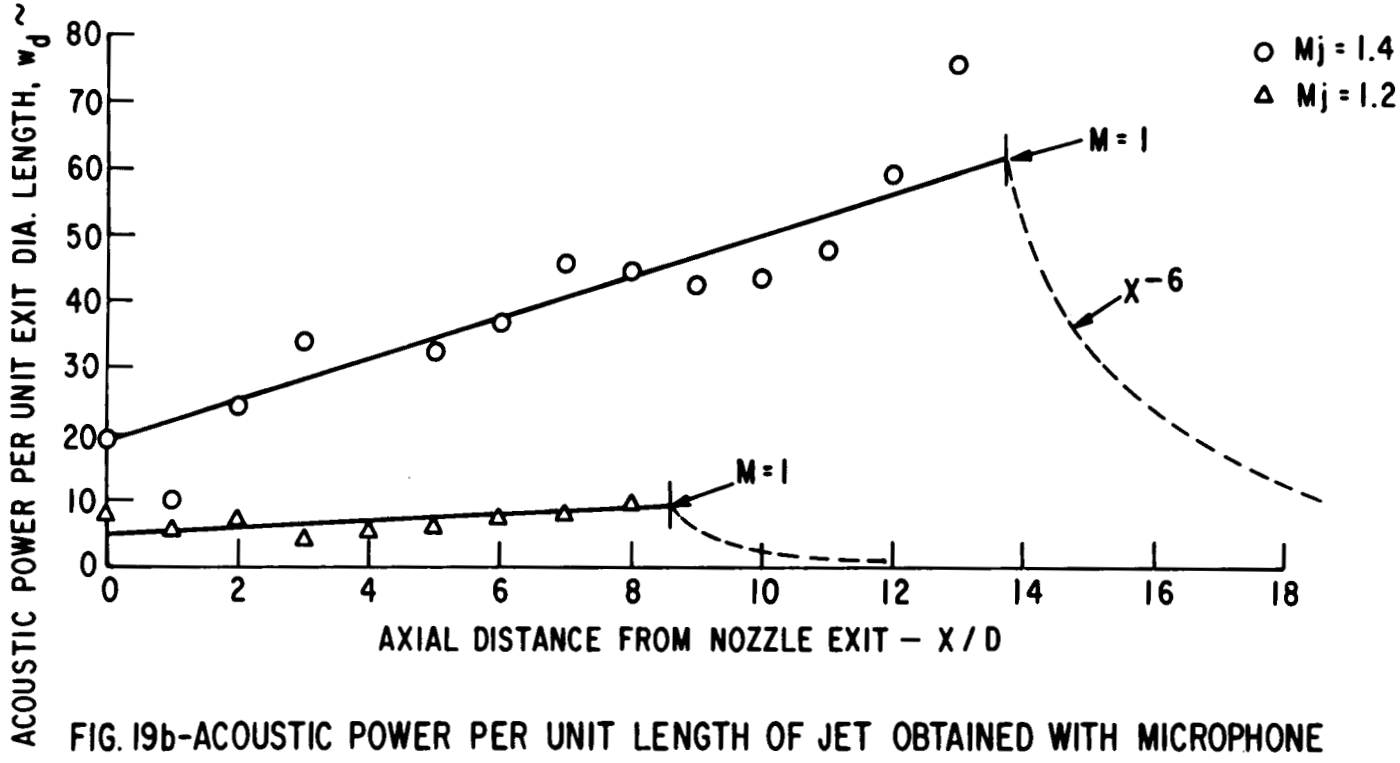

FIG. 19b-ACOUSTIC POWER PER UNIT LENGTH OF JET OBTAINED WITH MICROPHONE TRAVERSE PARALLEL TO JET AXIS AT TWO NOZZLE DIAMETERS FROM NOZZLE PERIPHERY.

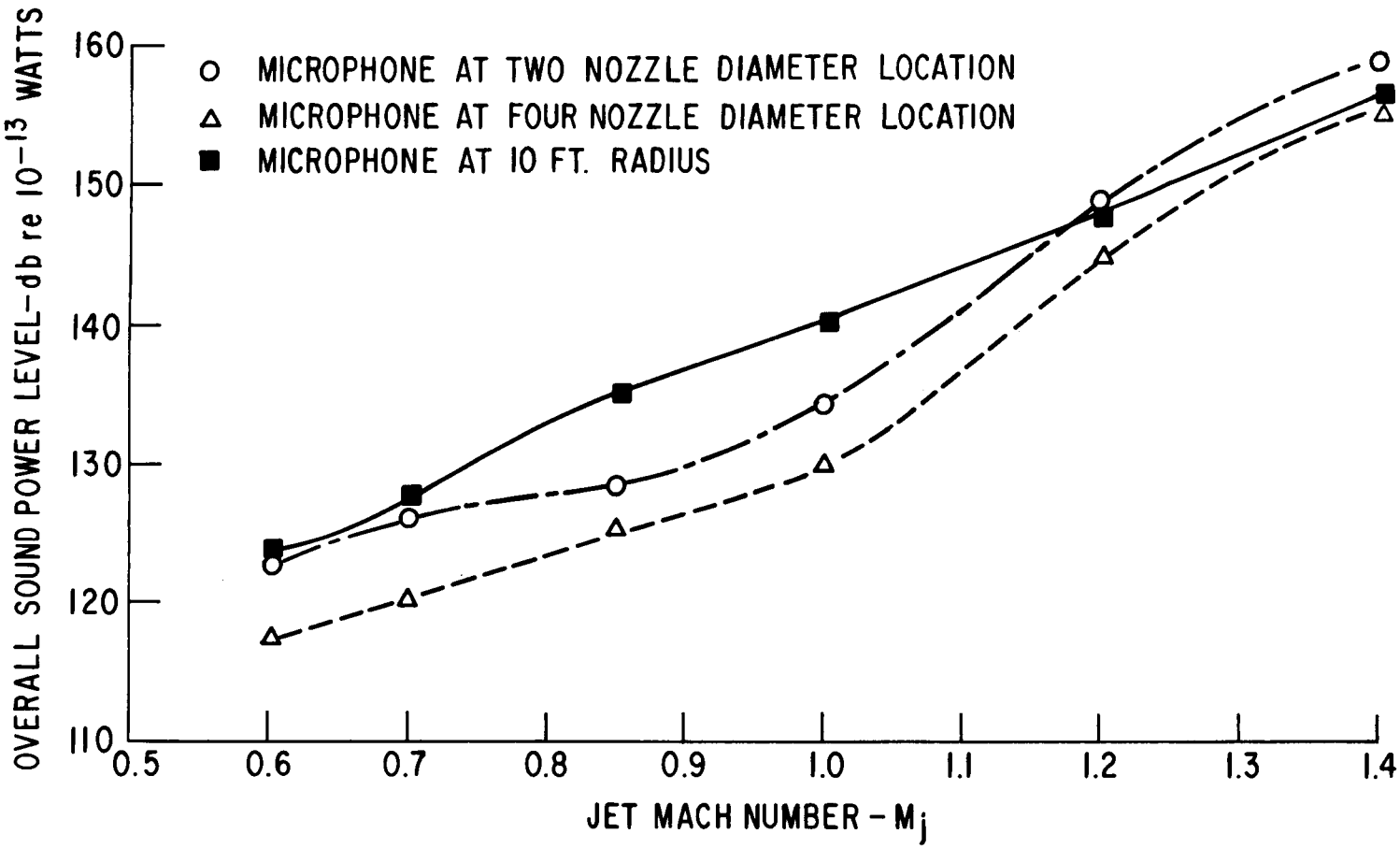

FIG. 20-OVERALL SOUND POWER LEVEL FOR CONVERGENT NOZZLE AT VARIOUS MACH NUMBERS

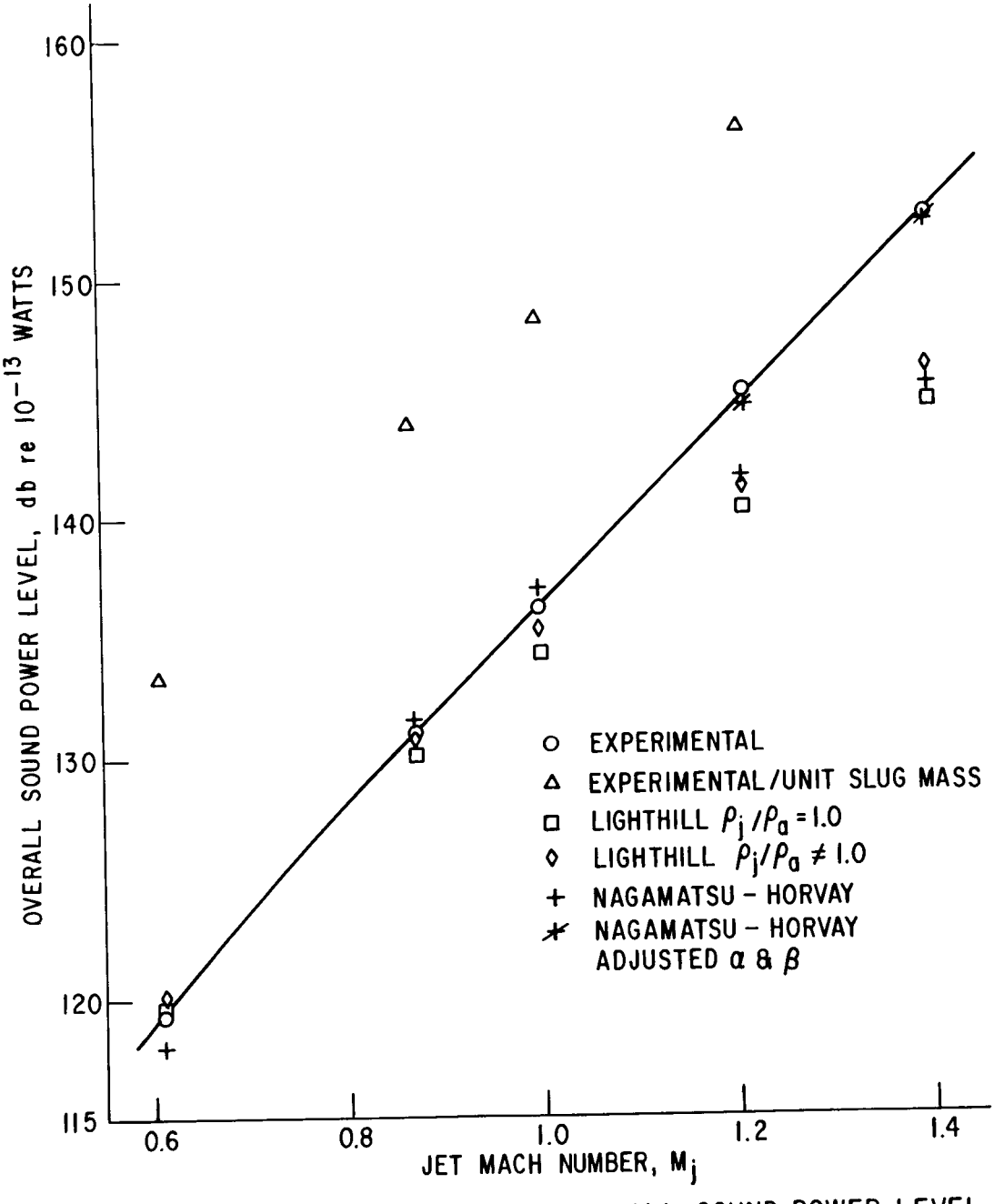

FIG.21-COMPARISON OF EXPERIMENTAL OVERALL SOUND POWER LEVEL FOR CONVERGENT NOZZLE WITH PREDICTIONS OF LIGHTHILL & NAGAMATSU-HORVAY THEORIES.

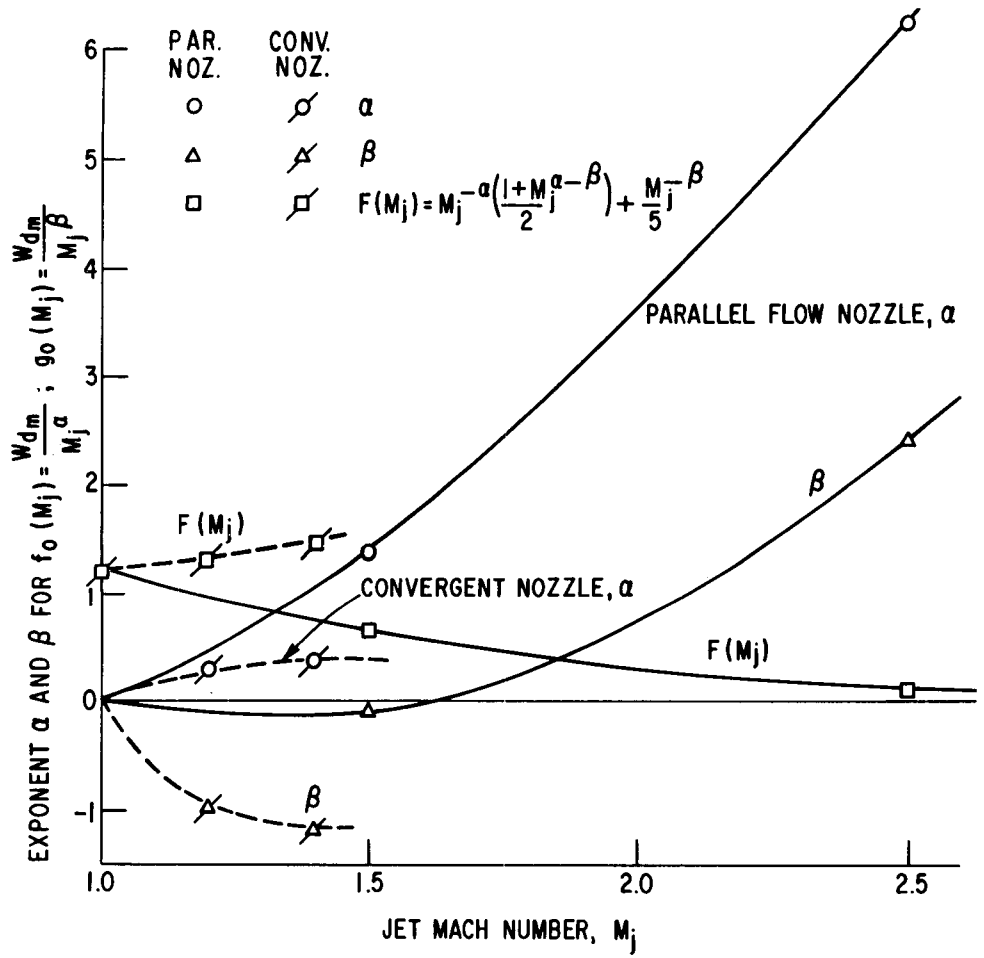

FIG. 22-VALUES OF EXPONENTS α AND β OF NAGAMATSU-HORVAY SUPERSONIC JET NOISE THEORY AS FUNCTION OF JET MACH NUMBER FOR PARALLEL FLOW AND CONVERGENT NOZZLE WITH $T_{tj} = 520°R$.

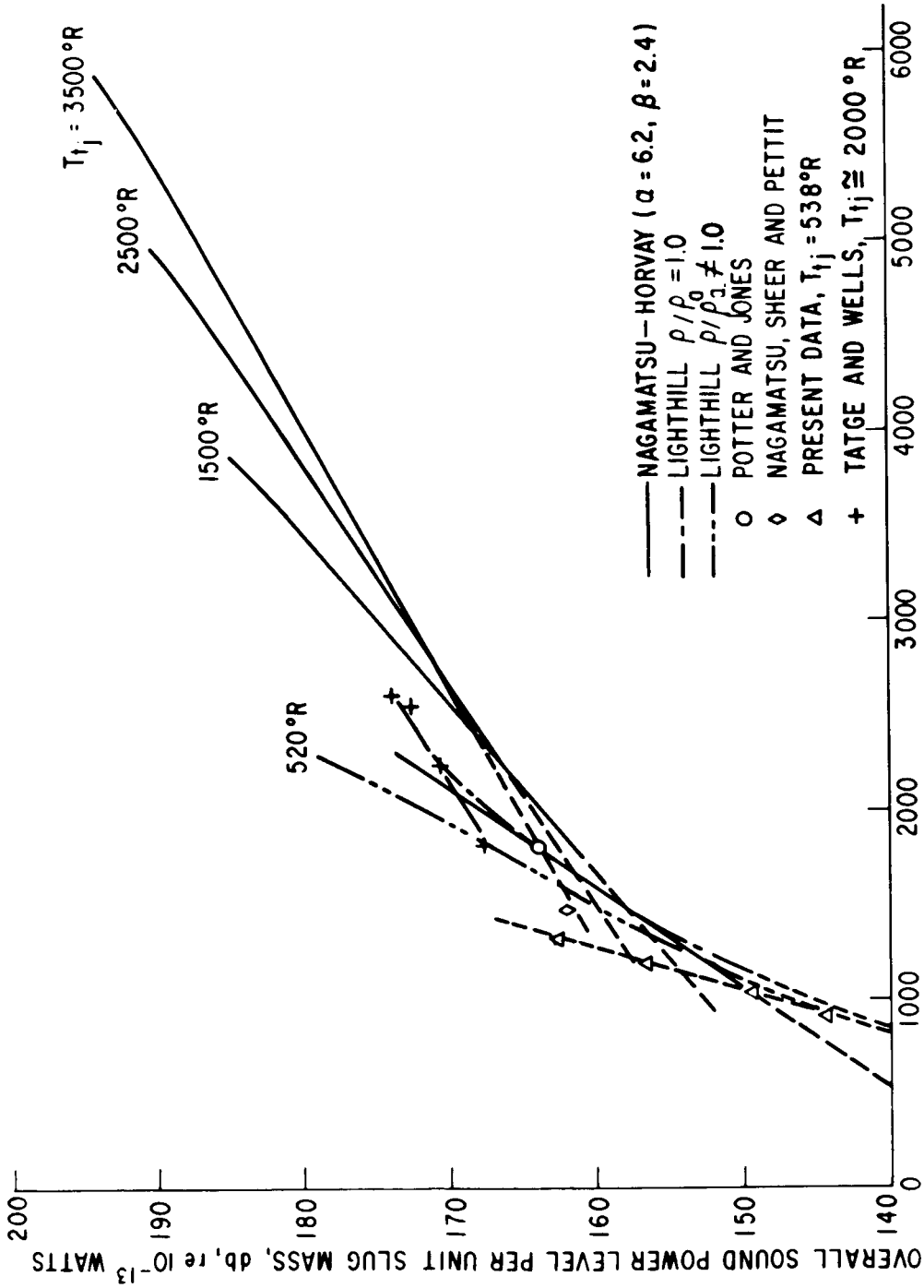

FIG. 23-OVERALL SOUND POWER LEVEL IN db PER UNIT SLUG MASS AS FUNCTION OF JET VELOCITY